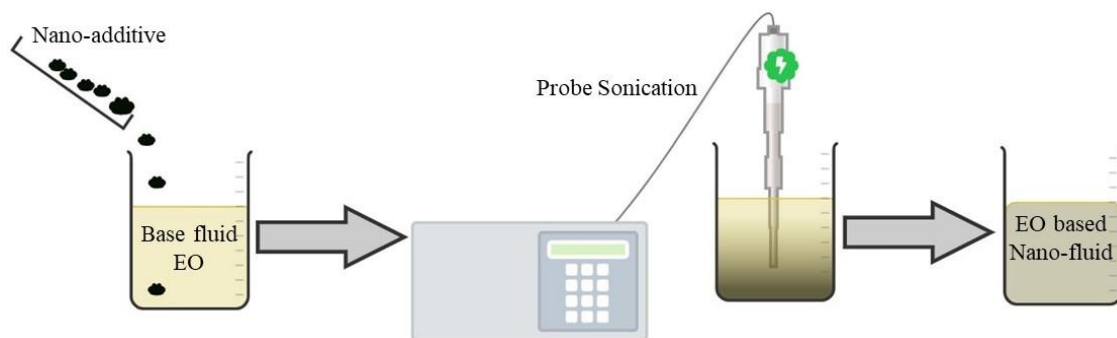


**Chapter 5**  
**Engine oil-based nanofluids containing**  
**Al<sub>2</sub>O<sub>3</sub>, ZnO, GNP and MWCNT**  
**nano-additives**

## 5.1: Preparation of engine oil-based nanofluids containing $\text{Al}_2\text{O}_3$ , $\text{ZnO}$ , $\text{GNP}$ and $\text{MWCNT}$ nano-additives

Dispersing nano-additives in a base fluid requires careful attention to develop an aggregate-free, stable liquid suspension that remains free from deposition over an extended period. The engine oil (EO) based nanofluid samples were prepared by incorporating nano-additive powders into EO using a two-step process. Initially, the nano-additives were weighed using an analytical balance (Mettler Toledo XSR105) with a precision of  $\pm 0.02$  mg to achieve the desired weight % of 0.05, 0.1, 0.2, and 0.5 at relevant quantity of EO. The nano-additive dispersed EO was sonicated using a high-power ultrasonication probe (Leela Sonic) with an output power of 500 watts and a frequency of 20 kHz for 3 hours in pulse mode to achieve a stable and homogeneous EO-based nanofluid. Fig. 5.1 illustrates the typical preparation process of EO-based nanofluids containing different nano-additives. Fig. 5.2 to 5.6 display real images of the nano-additives ( $\text{Al}_2\text{O}_3$ ,  $\text{ZnO}$ ,  $\text{GNP}$ , and  $\text{MWCNT}$ ) and their dispersion into the EO base fluid.



**Fig. 5.1:** Preparation of engine oil (EO)-based nanofluids containing nano-additives.

Following EO-based nanofluids prepared by dispersing nano-additives:

1. EO-based nanofluids containing  $\text{Al}_2\text{O}_3$  nano-additives ( **$\text{Al}_2\text{O}_3/\text{EO}$  nanofluids**),
2. EO-based nanofluids containing  $\text{ZnO}$  nano-additives ( **$\text{ZnO}/\text{EO}$  nanofluids**),
3. EO-based nanofluids containing  $\text{GNP}$  nano-additives ( **$\text{GNP}/\text{EO}$  nanofluids**), and
4. EO-based nanofluids containing  $\text{MWCNT}$  nano-additives ( **$\text{MWCNT}/\text{EO}$  nanofluids**)

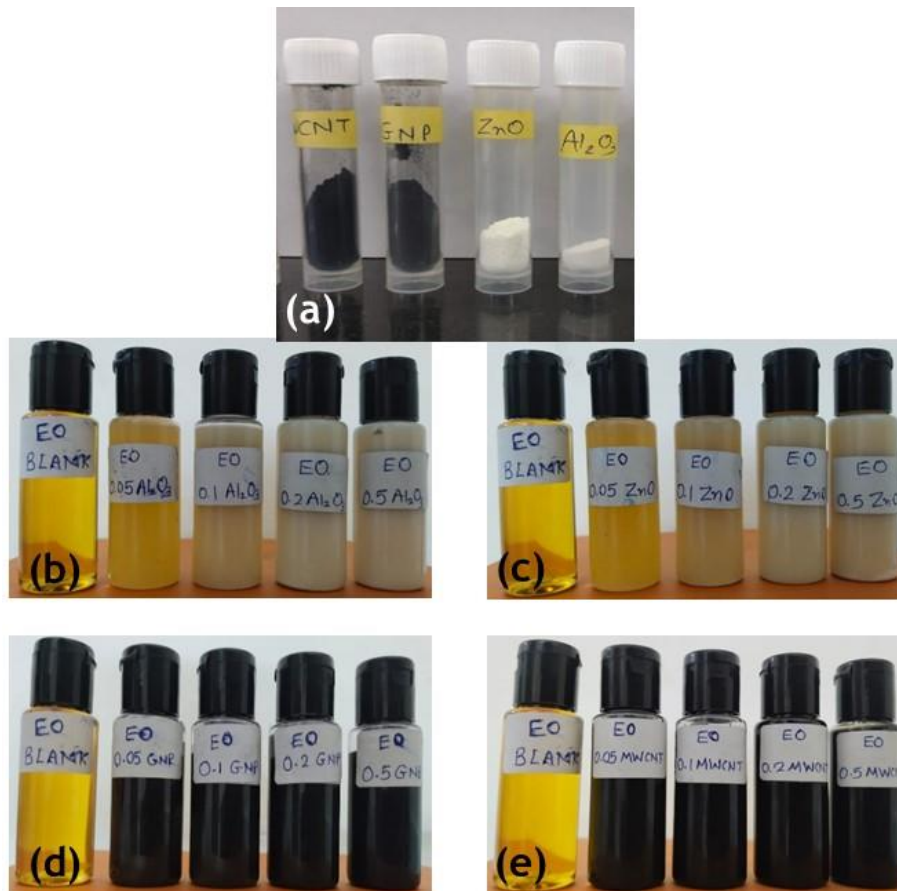


**Fig. 5.2:** (a) Nano-additives ( $Al_2O_3$ , ZnO, GNP and MWCNT) used to prepare EO-based nanofluids. (b)  $Al_2O_3$ /EO nanofluids with different  $Al_2O_3$  concentrations, (c) ZnO/EO nanofluids with different ZnO concentrations, (d) GNP/EO nanofluids with different GNP concentrations, and (e) MWCNT/EO nanofluids with different MWCNT concentrations.

## 5.2: EO-based nanofluid containing Al<sub>2</sub>O<sub>3</sub> nano-additives

### (Al<sub>2</sub>O<sub>3</sub>/EO nanofluids)

In this study, a comprehensive rheological investigation was carried out to assess the dynamic viscosity of both pure EO and Al<sub>2</sub>O<sub>3</sub>/EO nanofluids under different Al<sub>2</sub>O<sub>3</sub> nano-additive concentrations, shear rates, and temperature conditions. The main focus was to understand the influence of Al<sub>2</sub>O<sub>3</sub> weight % and temperature on the dynamic viscosity and thermal conductivity of Al<sub>2</sub>O<sub>3</sub>/EO nanofluids. The obtained results shed light on the potential applications of Al<sub>2</sub>O<sub>3</sub>/EO nanofluids as efficient EOs.

#### 5.2.1: Flow characteristics of Al<sub>2</sub>O<sub>3</sub>/EO nanofluids using rheometry

Fig. 5.3 exhibits the impact of shear rate on the dynamic viscosity of Al<sub>2</sub>O<sub>3</sub>/EO nanofluids at different Al<sub>2</sub>O<sub>3</sub> weight % and temperatures: 40°C to 100°C. The findings indicate that the dynamic viscosity of both Al<sub>2</sub>O<sub>3</sub>/EO nanofluids and pure EO decreases initially with increasing shear rates at 40°C for all nano-additive concentrations. This shows initial shear thinning behaviour of non-newtonian fluid. At higher shear rates and at all temperatures, all fluids exhibit linear behaviour indicating newtonian fluid characteristic i.e., fluids have a constant viscosity regardless of the shear rates applied. The experimental findings suggest a newtonian fluid behaviour for both Al<sub>2</sub>O<sub>3</sub>/EO nanofluids and pure EO at higher shear rates at any temperature within the experimental range. However, at higher shear rates and higher temperature, nanofluids with higher Al<sub>2</sub>O<sub>3</sub> weight % exhibit a slight pseudoplastic i.e., shear-thinning behaviour relative to nanofluids with lower Al<sub>2</sub>O<sub>3</sub> weight %. This observation suggests that increased Al<sub>2</sub>O<sub>3</sub> concentration, represented by weight %, has a notable impact on enhancing shear thinning in both Al<sub>2</sub>O<sub>3</sub>/EO nanofluids and pure EO.

Fig. 5.4 presents the effect of Al<sub>2</sub>O<sub>3</sub> weight% on dynamic viscosity of nanofluids at a constant temperature. The Al<sub>2</sub>O<sub>3</sub> concentration has a significant influence on dynamic viscosity within the shear rate of 100 to 5000 s<sup>-1</sup> at 40°C and 60°C temperatures. At these temperatures dynamic viscosity of all nanofluids increases slightly with increasing Al<sub>2</sub>O<sub>3</sub> nano-additive concentration. However, at higher temperatures i.e., 80°C and 100°C, rate of increase in dynamic viscosity with increasing Al<sub>2</sub>O<sub>3</sub> nano-additive concentration became very less at all shear rates. At lower temperatures (40°C and 60°C), increased dynamic viscosity of nanofluids attributed to the enhanced resistance to flow depicted by the

presence of solid  $\text{Al}_2\text{O}_3$  nano-additive in the EO fluid. Consequently, increasing the  $\text{Al}_2\text{O}_3$  nano-additive concentration results in higher nanofluid viscosity. However, it's important to note that the dynamic viscosity does not always increase significantly with concentration. For instance, in Fig. 5.4 (c) and (d), the increase in dynamic viscosity is negligible as relative to lower temperature of  $40^\circ\text{C}$ .

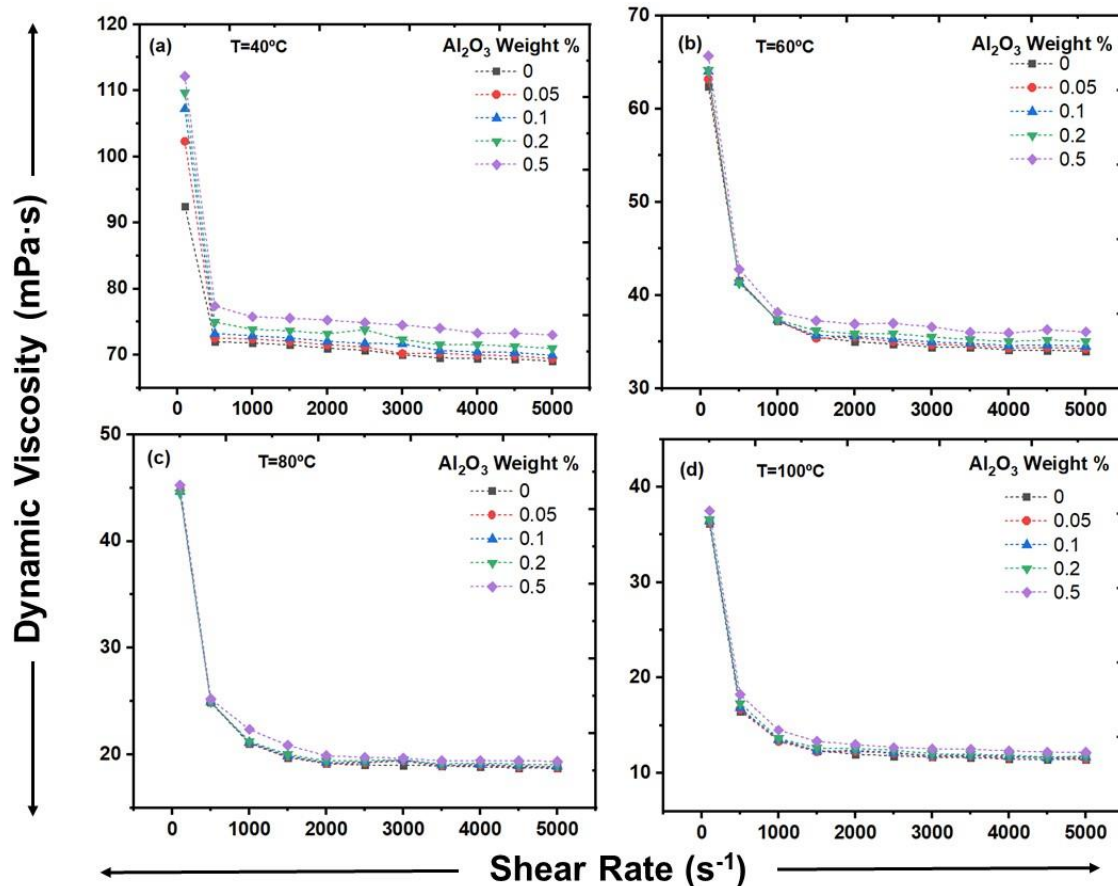


**Fig. 5.3 (a-d):** Effect of shear rate on dynamic viscosity of  $\text{Al}_2\text{O}_3/\text{EO}$  nanofluids at different mass fraction.

Fig. 5.5 depicts the effect of temperature on the dynamic viscosity of pure EO and  $\text{Al}_2\text{O}_3/\text{EO}$  nanofluids with varying nano-additive  $\text{Al}_2\text{O}_3$  weight %. This analysis is conducted at constant shear rates of  $500 \text{ s}^{-1}$  and  $5000 \text{ s}^{-1}$ . As the temperature rises from  $40^\circ\text{C}$  to  $100^\circ\text{C}$ , the dynamic viscosity decreases for both EO fluids and  $\text{Al}_2\text{O}_3/\text{EO}$  nanofluids. For instance, at a shear rate of  $500 \text{ s}^{-1}$ , the  $\text{Al}_2\text{O}_3/\text{EO}$  nanofluid with a 0.5 weight%  $\text{Al}_2\text{O}_3$  concentration shows a viscosity of  $77 \text{ mPa}\cdot\text{s}$  at  $40^\circ\text{C}$ , which decreases to  $18 \text{ mPa}\cdot\text{s}$  at  $100^\circ\text{C}$ . Similar trends are observed for other nano-additive  $\text{Al}_2\text{O}_3$  weight %. These observations can be attributed to a decrease in intermolecular adhesion forces as temperature rises. Moreover, the effect of solid nano-additive  $\text{Al}_2\text{O}_3$  concentration on

dynamic viscosity is more prominent at lower temperatures. However, this influence becomes less significant as the temperature increases.

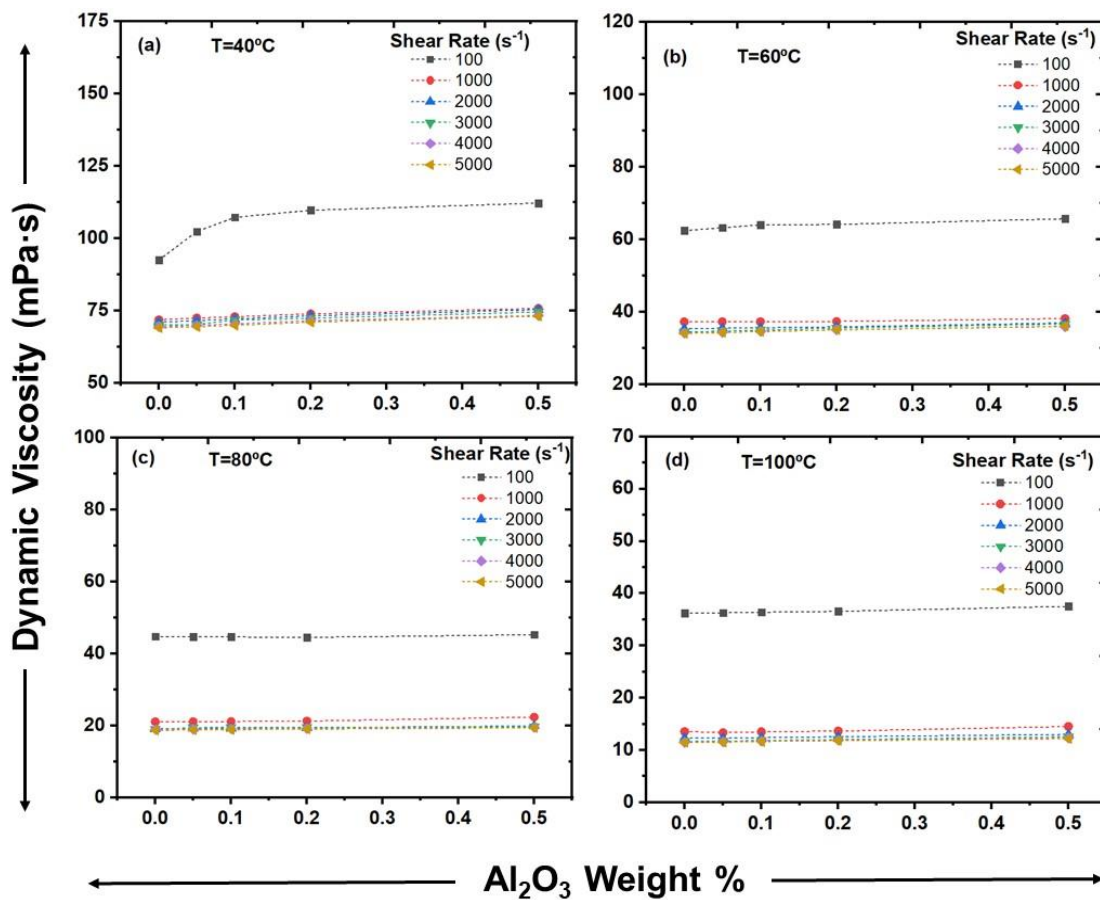


Fig. 5.4 (a-d): Effect of solid mass fractions on dynamic viscosity of  $\text{Al}_2\text{O}_3/\text{EO}$  nanofluids at different shear rates.

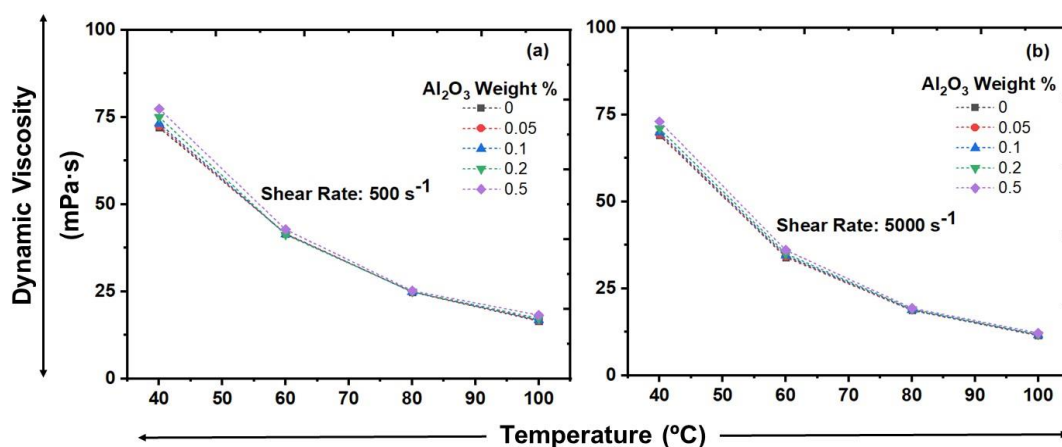
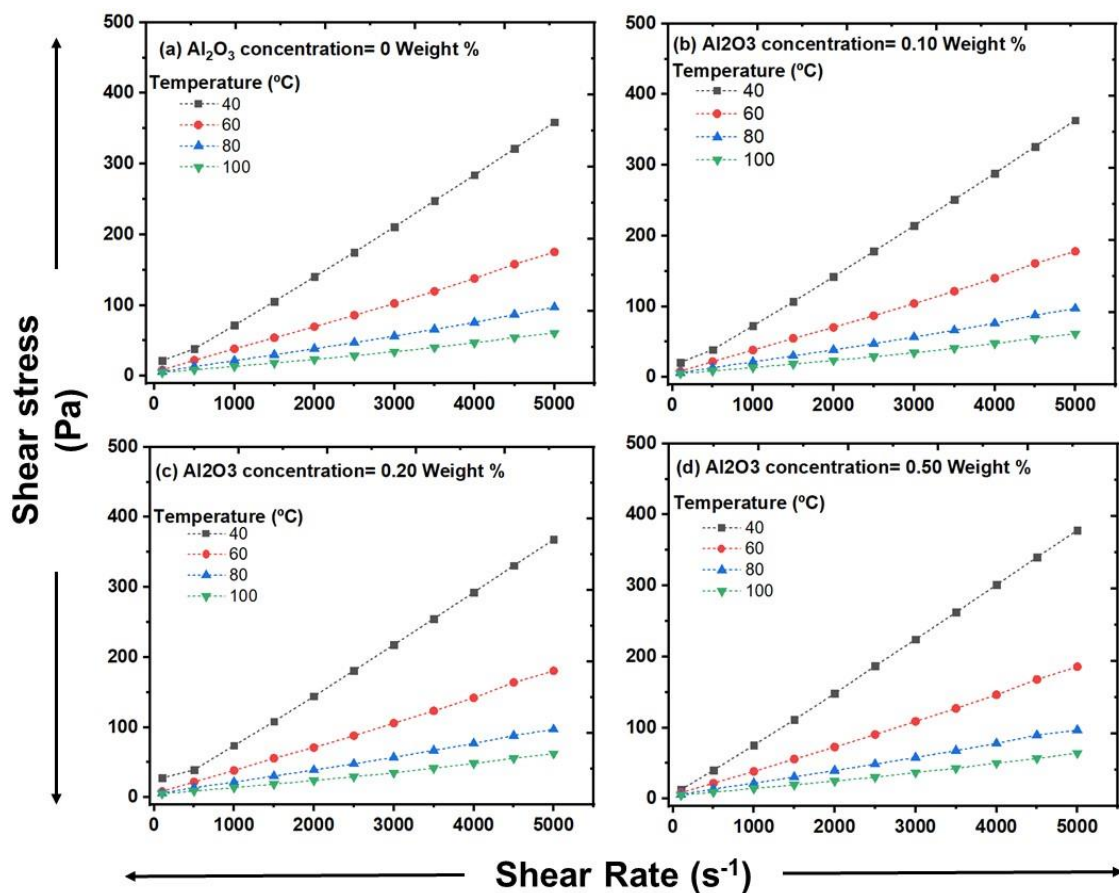


Fig. 5.5 (a-b): Effect of temperature on the dynamic viscosity of  $\text{Al}_2\text{O}_3/\text{EO}$  nanofluids at different solid mass fractions.

In Fig. 5.6 (a-d), the correlation between shear rate & shear stress of  $\text{Al}_2\text{O}_3/\text{EO}$  nanofluid is depicted at different temperatures for various  $\text{Al}_2\text{O}_3$  weight % (0.0, 0.05, 0.1, 0.2, and 0.5). The figures demonstrate that shear stress increases as shear rate increases across all temperatures. To determine the flow behaviour of the fluid, whether it follows newtonian flow or non-newtonian flow, the Ostwald-de-Waele (OdW) model is employed using Equation (1) as discussed in introduction part of chapter 1 [1-3]. In this analysis, fitting of power law curves was applied to the shear stress vs. shear rate curve to find the values of consistency index (m) and power law index (n). The obtained values of m and n are displayed in Table 5.1.



**Fig. 5.6 (a-d):** Shear stress vs. shear rate at various temperature for  $\text{Al}_2\text{O}_3/\text{EO}$  nanofluids.

As presented in Fig. 5.7, the values of power law index (n) are close to or equal to one at 40°C for all nano-additive  $\text{Al}_2\text{O}_3$  weight % and temperature ranges of the nanofluids, indicating a newtonian fluid flow behaviour. The values of n for all nano-additive  $\text{Al}_2\text{O}_3$  weight % and temperatures (80°C and 100°C) of the nanofluids are less than 1, suggesting a pseudo plastic non-newtonian fluid flow behaviour. At 60°C with

increasing nano-additive Al<sub>2</sub>O<sub>3</sub> concentration in EO, different flow characteristics are observed. At lower concentration 0.05 weight %, EO and Al<sub>2</sub>O<sub>3</sub>/EO nanofluids show pseudo plastic non-newtonian fluid behaviour. Above 0.05 weight % concentration, Al<sub>2</sub>O<sub>3</sub>/EO nanofluid show newtonian fluid behaviour. This observation suggests that at higher temperatures of 80°C and 100°C, Al<sub>2</sub>O<sub>3</sub>/EO nanofluids shows different flow behaviours than lower temperatures 40°C and 60°C depending on nano-additive Al<sub>2</sub>O<sub>3</sub> concentration in base fluid. This may help in designing the Al<sub>2</sub>O<sub>3</sub>/EO nanofluid as per flow behaviour requirement in different type of EO applications.

**Table 5.1:** The power law index (n) and consistency index (m) values of Al<sub>2</sub>O<sub>3</sub>/EO nanofluids.

Temperature (°C)	Indexes	Al <sub>2</sub> O <sub>3</sub> concentration (Weight %)				
		0	0.05	0.1	0.2	0.5
40	m	66	67	68	72	71
	n	1.0083	1.0084	1.0067	1.0014	1.0074
60	m	43	43	42	40	37
	n	0.9755	0.9762	0.9807	0.9857	0.9993
80	m	26	26	27	29	32
	n	0.9652	0.9631	0.9592	0.9533	0.9415
100	m	14	15	15	15	17
	n	0.9779	0.9748	0.9777	0.9774	0.9667

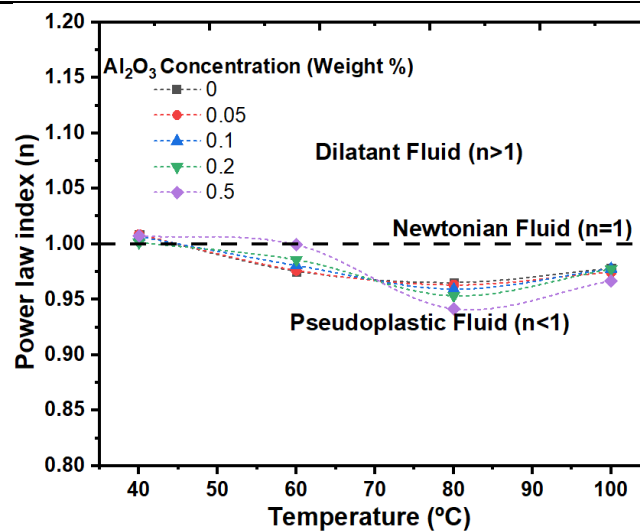


**Fig. 5.7:** Power law index for different solid mass fractions and temperature for Al<sub>2</sub>O<sub>3</sub>/EO nanofluids.

Furthermore, Fig. 5.8 depicts the relationship between the nanofluids' temperature & the consistency index (m) for different Al<sub>2</sub>O<sub>3</sub> weight%. The results clearly demonstrate m value declines with increasing temperature. This indicates that as the temperature rises, the fluid's mobility decreases, resulting in reduced flow resistance. It is noteworthy that the

consistency index does not change with the  $\text{Al}_2\text{O}_3$  concentration at higher temperatures. This observation confirms that higher  $\text{Al}_2\text{O}_3$  concentrations in the base fluid do not substantially increase resistance to fluid flow.

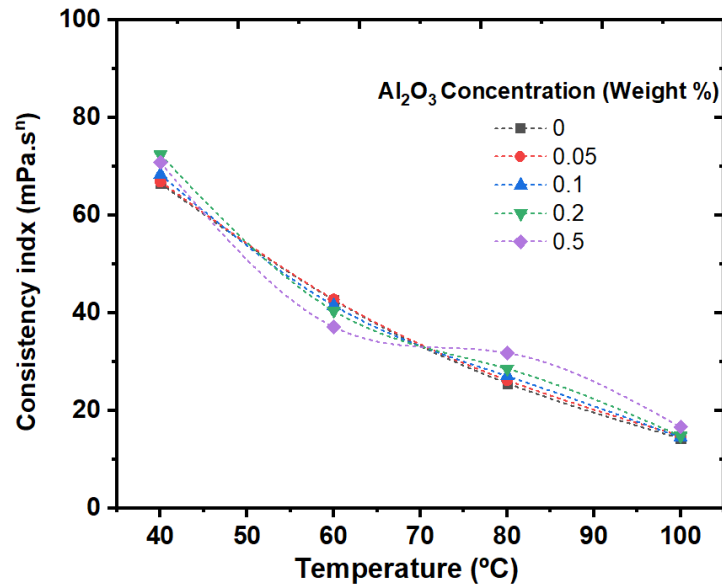


**Fig. 5.8:** Consistency index for different solid mass fractions and temperatures for  $\text{Al}_2\text{O}_3/\text{EO}$  nanofluids.

### 5.2.2: Thermal conductivity characteristics of $\text{Al}_2\text{O}_3/\text{EO}$ nanofluids

In Fig. 5.9 (a), the thermal conductivity of pure EO and  $\text{Al}_2\text{O}_3/\text{EO}$  nanofluid is shown for  $\text{Al}_2\text{O}_3$  concentration over a temperature: 30°C to 70°C. The data reveal that the thermal conductivity improves with an increase in the  $\text{Al}_2\text{O}_3$  concentration. Moreover, at higher  $\text{Al}_2\text{O}_3$  concentrations, thermal conductivity exhibits a steeper slope, indicating a more pronounced enhancement. This increased thermal conductivity is attributed to higher heat conductivity of  $\text{Al}_2\text{O}_3$  incorporated into the EO fluid. It is noteworthy to notice, thermal conductivity of both EO fluid and the  $\text{Al}_2\text{O}_3/\text{EO}$  nanofluid with a 0.05 weight %  $\text{Al}_2\text{O}_3$  concentration diminish as the temperature increases. However, a thermal conductivity reversal behaviour is observed at a  $\text{Al}_2\text{O}_3$  concentration above 0.1 weight% in the BO. In this case, the thermal conductivity of  $\text{Al}_2\text{O}_3/\text{EO}$  nanofluids increases with rising temperature. This is explained by the increased interaction and spread of  $\text{Al}_2\text{O}_3$  particles within the EO fluid at higher temperatures. These changes are driven by the energy transfer between the layers of the nanofluid, resulting in enhanced heat transfer capabilities of the nanofluids [4-6]. Overall, the finding shows that  $\text{Al}_2\text{O}_3/\text{EO}$  nanofluids have enhanced thermal conductivity relative to pure EO fluid.

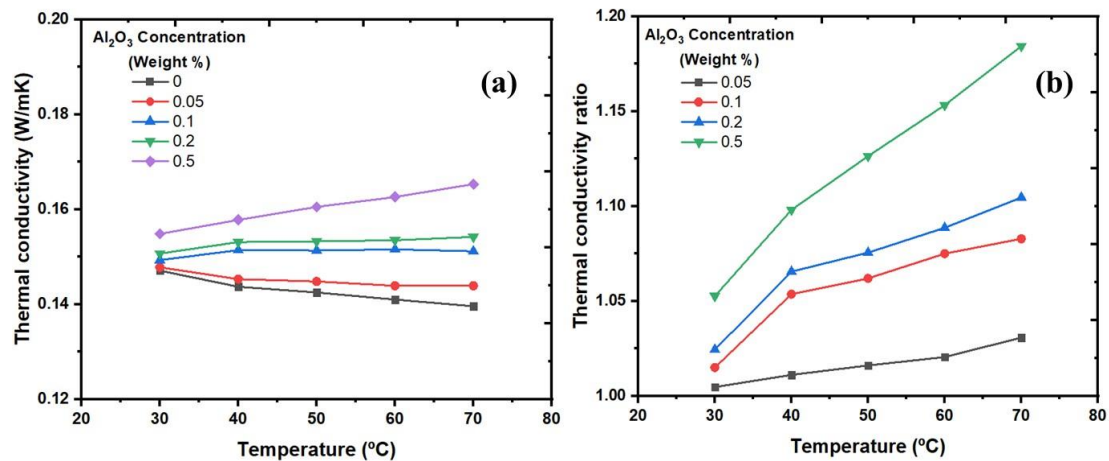


**Fig. 5.9:** (a) Thermal conductivity of  $Al_2O_3$ /EO nanofluids, and (b) thermal conductivity ratio of  $Al_2O_3$ /EO nanofluids.

The thermal conductivity ratio of the  $Al_2O_3$ /EO nanofluid relative to the EO base fluid is shown in Fig. 5.9 (b). The ratio increases with rising temperature. At low  $Al_2O_3$  weight %, there are minimal increases in thermal conductivity because of lower concentration of  $Al_2O_3$  in the fluid. However, as the  $Al_2O_3$  concentration increases, the number of nanoparticles & their collisions also increases, resulting in effective heat transfer between fluid layers [7, 8]. This results in greater thermal conductivity values for the  $Al_2O_3$ /EO nanofluid relative to the base EO fluid. In present work, thermal conductivity of the  $Al_2O_3$ /EO nanofluid increased by 18.4% at 70°C for a  $Al_2O_3$  concentration of 0.5 weight%. This significant enhancement demonstrates the capability of  $Al_2O_3$ /EO nanofluids to enhance heat transfer performance in various EO applications.

### 5.3: EO-based nanofluid containing ZnO nano-additives (ZnO/EO nanofluids)

In this study, a comprehensive rheological investigation was carried out to assess the dynamic viscosity of both pure EO and ZnO/EO nanofluids under different ZnO nano-additive concentrations, shear rates, and temperature conditions. The main focus was to understand the influence of ZnO weight % and temperature on the dynamic viscosity and thermal conductivity of ZnO/EO nanofluids. The obtained results shed light on the potential applications of ZnO/EO nanofluids as efficient EOs.

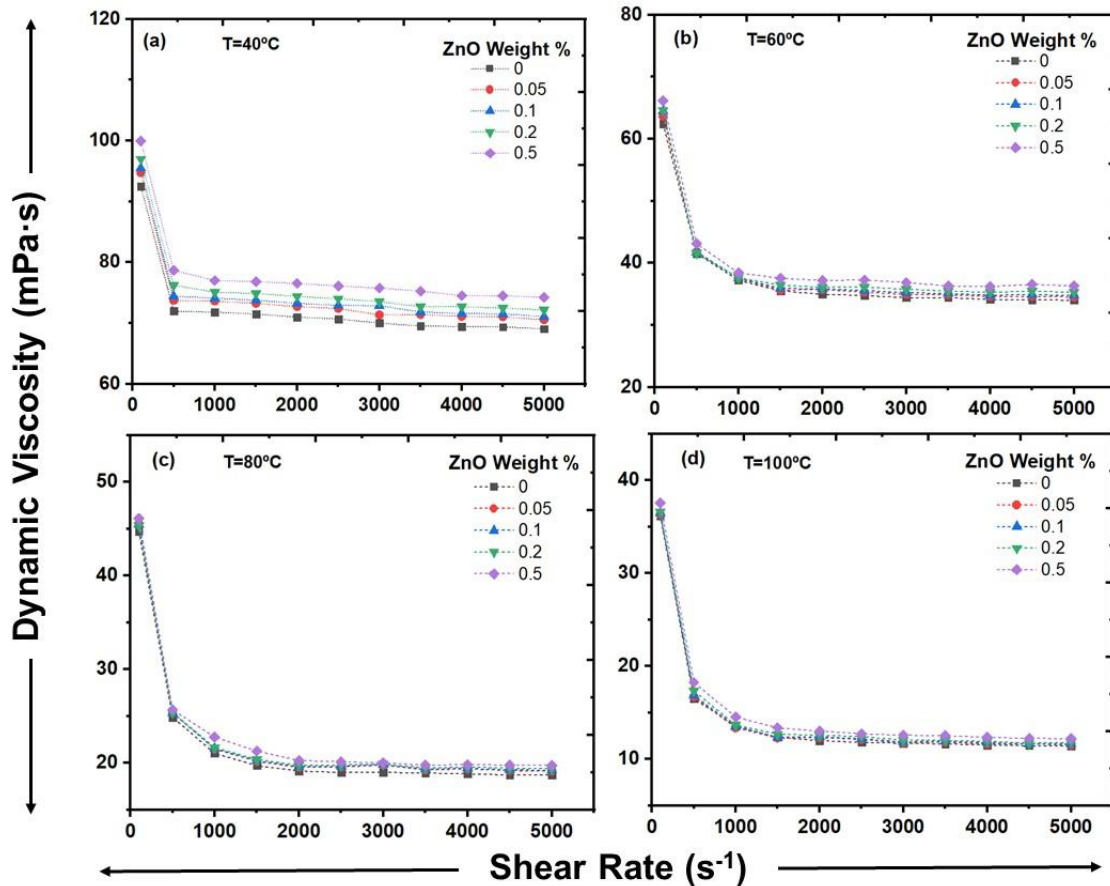
#### 5.3.1: Flow characteristics of ZnO/EO nanofluids using rheometry

Fig. 5.10 exhibits the impact of shear rate on the dynamic viscosity of ZnO/EO nanofluids at different ZnO weight % and temperatures: 40°C to 100°C. The findings indicate that the dynamic viscosity of both ZnO/EO nanofluids and pure EO decreases initially with increasing shear rates at all measured temperature range for all ZnO nano-additive concentrations. This shows initial shear thinning behaviour of non-newtonian fluid. At higher shear rates and at all temperatures, all fluids exhibit linear behaviour indicating newtonian fluid characteristic i.e., fluids have a constant viscosity regardless of the shear rates applied. The experimental findings suggest a newtonian fluid behaviour for both ZnO/EO nanofluids and pure EO at higher shear rates at any temperature within the experimental range. However, at higher shear rates and higher temperature, nanofluids with higher ZnO weight % exhibit a mild pseudoplastic i.e., shear-thinning behaviour relative to nanofluids with lower ZnO weight %. This observation suggests that increased ZnO concentration, represented by weight %, has a notable impact on enhancing shear thinning in both ZnO/EO nanofluids and pure EO.

Fig. 5.11 presents the effect of ZnO weight% on dynamic viscosity of constantly-temperated nanofluids. The ZnO concentration has a significant effect on the dynamic viscosity within the shear rate range of 100 to 5000  $s^{-1}$  at 40°C, 60 °C and 80°C temperatures. At these temperatures dynamic viscosity of all nanofluids increases slightly with increasing ZnO nano-additive concentration. However, at higher temperatures i.e., 100°C, rate of increase in dynamic viscosity with increasing ZnO nano-additive concentration became very less at all shear rates. At lower temperatures (40°C and 60°C), increased dynamic viscosity of nanofluids attributed to the enhanced resistance to flow

---

depicted by the presence of solid ZnO nano-additive in the EO fluid. Consequently, increasing the ZnO nano-additive concentration results in higher nanofluid viscosity. However, it's important to note that the dynamic viscosity does not always increase significantly with concentration. For instance, in Fig. 5.11 (d), the increase in dynamic viscosity is negligible as relative to lower temperature of 40°C.



**Fig. 5.10 (a-d):** Effect of shear rate on dynamic viscosity of ZnO/EO nanofluids at different mass fraction.

Fig. 5.12 depicts the influence of temperature on the dynamic viscosity of pure EO and ZnO/EO nanofluids with varying nano-additive ZnO weight %. This analysis is conducted at constant shear rates of  $500 \text{ s}^{-1}$  and  $5000 \text{ s}^{-1}$ . As the temperature rises from 40°C to 100°C, the dynamic viscosity decreases for both EO fluids and ZnO/EO nanofluids. For instance, at a shear rate of  $5000 \text{ s}^{-1}$ , the ZnO/EO nanofluid with a 0.5 weight% ZnO concentration shows a viscosity of 74 mPa·s at 40°C, which decreases to 12 mPa·s at 100°C. Similar trends are observed for other nano-additive ZnO weight %. These observations can be attributed to a decrease in intermolecular adhesion forces as temperature rises. Moreover, the effect of solid nano-additive ZnO concentration on

dynamic viscosity is more prominent at lower temperatures. However, results indicates that this influence not much significant as the temperature rises.

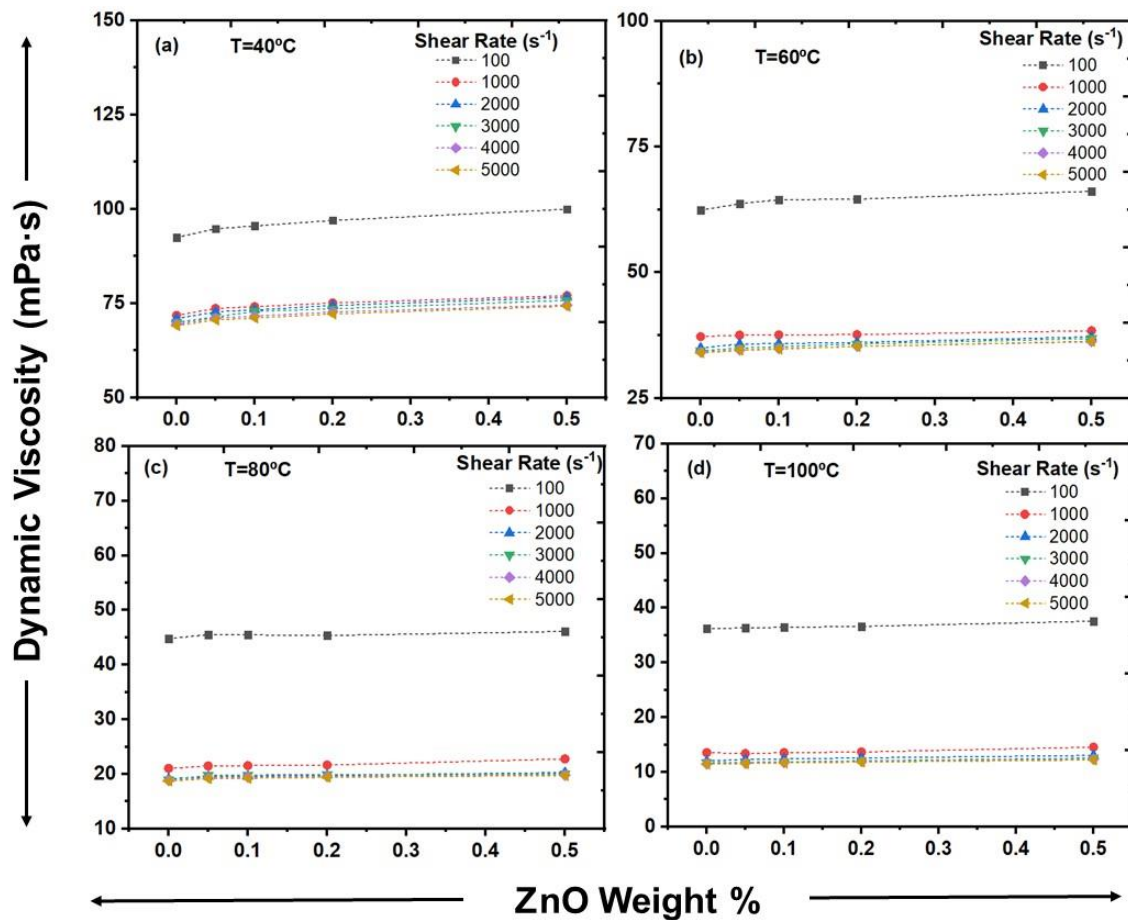


Fig. 5.11 (a-d): Effect of solid mass fractions on dynamic viscosity of ZnO/EO nanofluids at different shear rates.

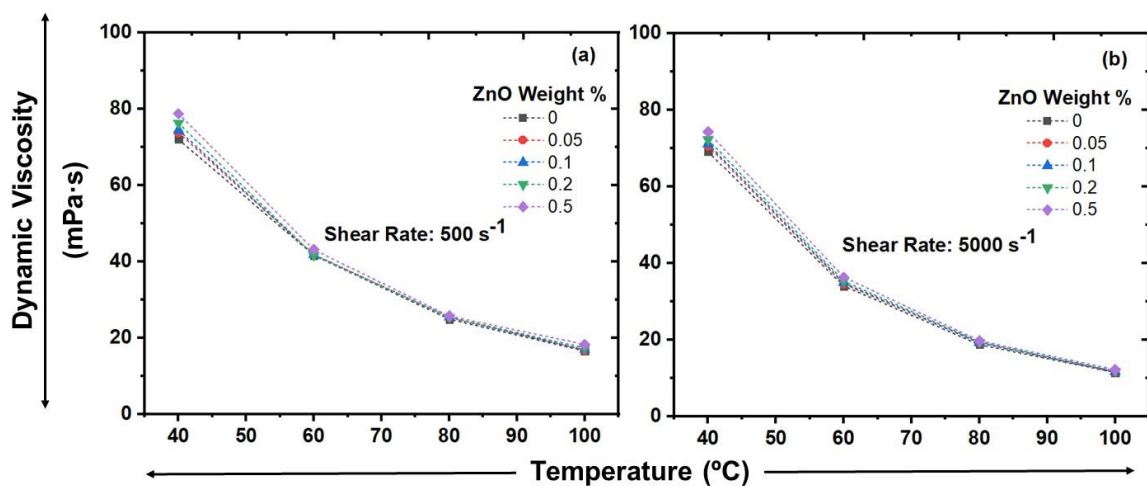
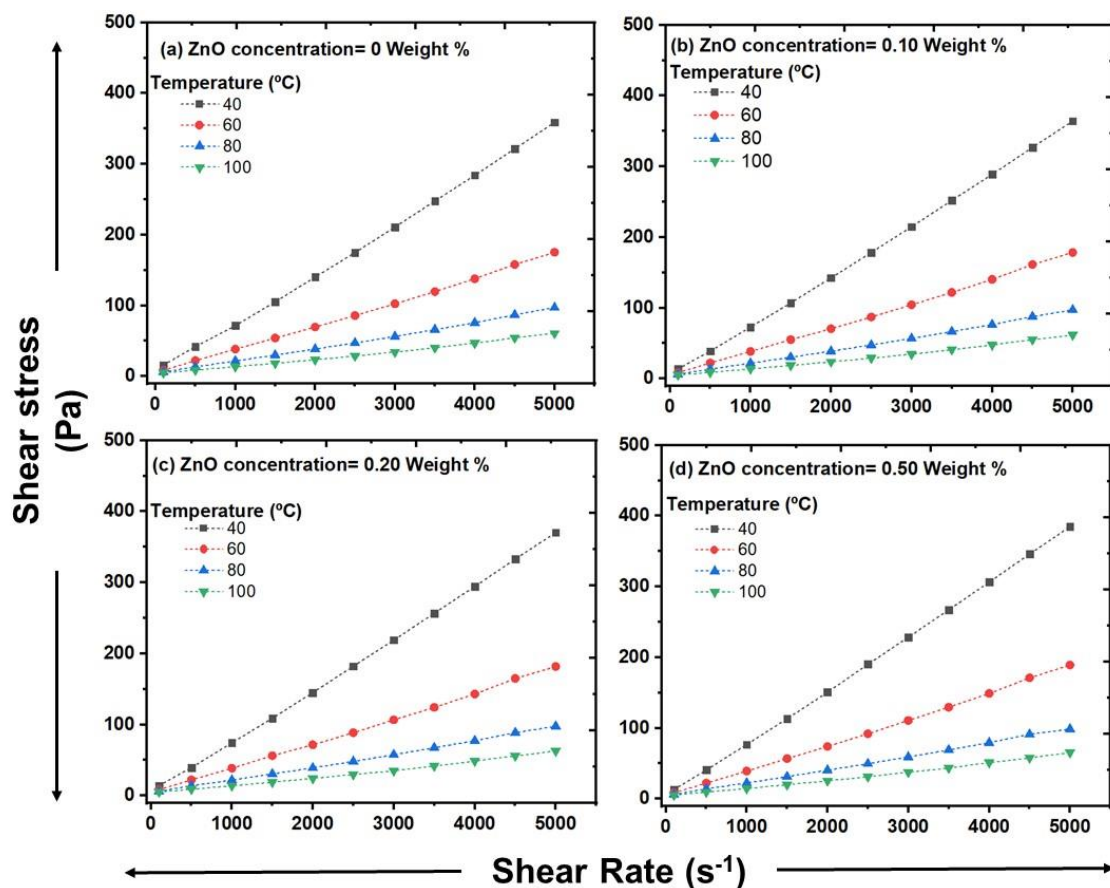


Fig. 5.12 (a-b): Effect of temperature on the dynamic viscosity of ZnO/EO nanofluids at different solid mass fractions.

In Fig. 5.13 (a-d), the correlation between shear rate & shear stress of ZnO/EO nanofluid is depicted at different temperatures for various ZnO weight % (0.0, 0.05, 0.1, 0.2, and 0.5). The figures demonstrate that shear stress increases as shear rate increases across all temperatures. To determine the flow behaviour of the fluid, whether it follows newtonian flow or non-newtonian flow, the Ostwald-de-Waele (OdW) model is employed using Equation (1) as discussed in introduction part of chapter 1 [1-3]. In this analysis, fitting of power law curves was applied to the shear stress vs. shear rate curve to find the values of consistency index (m) and power law index (n). The obtained values of m and n are displayed in Table 5.2.



**Fig. 5.13 (a-d):** Shear stress vs. shear rate at various temperature for ZnO/EO nanofluids.

As shown in Fig. 5.14, the values of power law index (n) are close to or equal to one at 40°C for all nano-additive ZnO weight % and temperature ranges of the nanofluids, indicating a newtonian fluid flow behaviour. The values of n for all nano-additive ZnO weight % and temperatures (80°C and 100°C) of the nanofluids are less than 1, suggesting a pseudo plastic non-newtonian fluid flow behaviour. At 60°C with increasing nano-

additive ZnO concentration in EO, different flow characteristics are observed. At lower concentration 0.05 weight %, EO and ZnO/EO nanofluids show pseudo plastic non-newtonian fluid behaviour. Above 0.05 weight % concentration, ZnO/EO nanofluid show newtonian fluid behaviour. This observation suggests that at higher temperatures of 80°C and 100°C, ZnO/EO nanofluids shows different flow behaviours than lower temperatures 40°C and 60°C depending on nano-additive ZnO concentration in base fluid. This may help in designing the ZnO/EO nanofluid as per flow behaviour requirement in different type of EO applications.

**Table 5.2:** The power law index (n) and consistency index (m) values of ZnO/EO nanofluids.

Temperature (°C)	Indexes	ZnO concentration (Weight %)				
		0	0.05	0.1	0.2	0.5
40	m	66	65	67	69	72
	n	1.0083	1.0120	1.0100	1.0078	1.0074
60	m	43	42	42	41	38
	n	0.9755	0.9781	0.9807	0.9857	0.9993
80	m	26	26	27	29	32
	n	0.9652	0.9622	0.9592	0.9533	0.9415
100	m	14	14	15	15	17
	n	0.9779	0.9778	0.9777	0.9774	0.9667

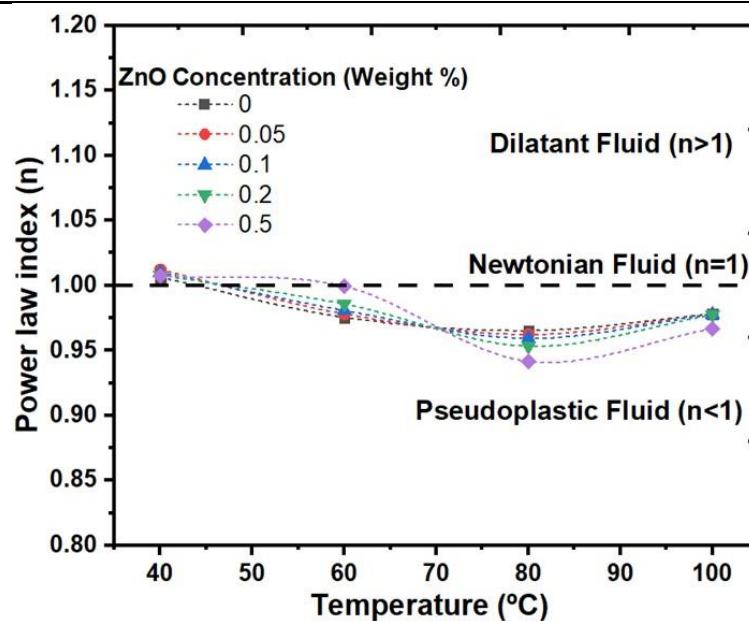


**Fig. 5.14:** Power law index for different solid mass fractions and temperature for ZnO/EO nanofluids.

Furthermore, Fig. 5.15 depicts the relationship between the nanofluids' temperature & the consistency index (m) for different ZnO weight%. The results clearly demonstrate m

value declines with increasing temperature. This indicates that as the temperature rises, the fluid's mobility decreases, resulting in reduced flow resistance. It is noteworthy that the consistency index does not change much with the ZnO concentration at higher temperatures. This observation confirms that higher ZnO concentrations in the base fluid do not substantially increase resistance to fluid flow.

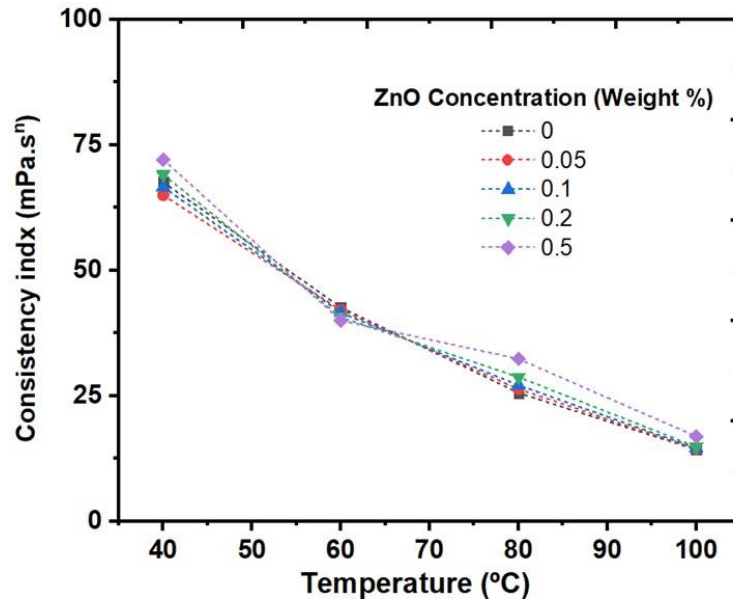


**Fig. 5.15:** Consistency index for different solid mass fractions and temperatures for ZnO/EO nanofluids.

### 5.3.2: Thermal conductivity characteristics of ZnO/EO nanofluids

In Fig. 5.16 (a), the thermal conductivity of pure EO and ZnO/EO nanofluid is shown for ZnO concentration over a temperature: 30°C to 70°C. The data reveal that the thermal conductivity improves with an increase in the ZnO concentration. Moreover, at higher ZnO concentrations, thermal conductivity exhibits a steeper slope, indicating a more pronounced enhancement. This increased thermal conductivity is attributed to higher heat conductivity of ZnO incorporated into the EO fluid. It is noteworthy to notice, thermal conductivity of both EO fluid and the ZnO/EO nanofluid with a 0.05 weight % ZnO concentration diminish as the temperature increases. However, a steady thermal conductivity behaviour is observed at a ZnO concentration 0.1 weight% in the BO. Further, a reversal in thermal conductivity behaviour is observed above a ZnO concentration 0.1 weight% in the BO. In this case, the thermal conductivity of ZnO/EO nanofluids increases with rising temperature. This is explained by the increased interaction and spread of ZnO particles within the EO fluid at higher temperatures. These changes are driven by the

energy transfer between the layers of the nanofluid, resulting in enhanced heat transfer capabilities of the nanofluids [4-6]. Overall, the finding shows that ZnO/EO nanofluids have enhanced thermal conductivity relative to the pure EO fluid.

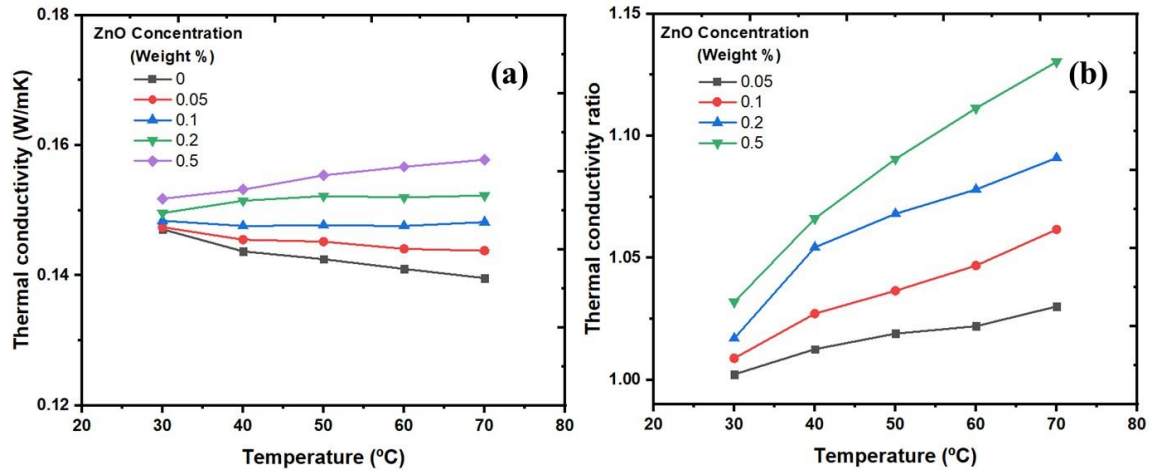


**Fig. 5.16:** (a) Thermal conductivity of ZnO/EO nanofluids, and (b) Thermal conductivity ratio of ZnO/EO nanofluids.

The thermal conductivity ratio of the ZnO/EO nanofluid relative to the EO base fluid is shown in Fig. 5.16 (b). The ratio increases with rising temperature. At low ZnO weight %, there are minimal increases in thermal conductivity because of lower concentration of ZnO in the fluid. However, as the ZnO concentration increases, the number of nanoparticles & their collisions also increases, resulting in effective heat transfer between fluid layers [7, 8]. This results in greater thermal conductivity values for the ZnO/EO nanofluid relative to the base EO fluid. In our study, the thermal conductivity of the ZnO/EO nanofluid increased by 13% at 70°C for a ZnO weight % of 0.5%. This significant enhancement demonstrates the capability of ZnO/EO nanofluids to enhance heat transfer performance in various EO applications.

## 5.4: EO-based nanofluid containing GNP nano-additives (GNP/EO nanofluids)

In this study, a comprehensive rheological investigation was carried out to assess the dynamic viscosity of both pure EO and GNP/EO nanofluids under different GNP nano-additive concentrations, shear rates, and temperature conditions. The main focus was to understand the influence of GNP weight % and temperature on the dynamic viscosity and thermal conductivity of GNP/EO nanofluids. The obtained results shed light on the potential applications of GNP/EO nanofluids as efficient EOs.

### 5.4.1: Flow characteristics of GNP/EO nanofluids using rheometry

Fig. 5.17 exhibits the impact of shear rate on the dynamic viscosity of GNP/EO nanofluids at different GNP weight % and temperatures: 40°C to 100°C. The findings indicate that the dynamic viscosity of both GNP/EO nanofluids and pure EO decreases initially with increasing shear rates at all temperatures for all GNP nano-additive concentrations. This shows initial shear thinning behaviour of non-newtonian fluid. At higher shear rates and at all temperatures, all fluids exhibit linear behaviour indicating newtonian fluid characteristic i.e., fluids have a constant viscosity regardless of the shear rates applied. The experimental findings suggest a newtonian fluid behaviour for both GNP/EO nanofluids and pure EO at higher shear rates at any temperature within the experimental range. However, at higher shear rates and higher temperature, nanofluids with higher GNP weight % exhibit a slight pseudoplastic i.e., shear-thinning behaviour relative to nanofluids with lower GNP weight %. This observation suggests that increased GNP concentration, represented by weight %, has a notable impact on enhancing shear thinning in both GNP/EO nanofluids and pure EO.

Fig. 5.18 presents the effect of GNP weight% on dynamic viscosity of constantly-temperated nanofluids. The GNP concentration has a significant effect on the dynamic viscosity within the shear rate range of 100 to 5000  $s^{-1}$  at 40°C and 60°C temperatures. At these temperatures dynamic viscosity of all nanofluids increases slightly with increasing GNP nano-additive concentration. However, at higher temperatures i.e., 80°C and 100°C, rate of increase in dynamic viscosity with increasing GNP nano-additive concentration became very less at all shear rates. At lower temperatures (40°C and 60°C), increased dynamic viscosity of nanofluids attributed to the enhanced resistance to flow depicted by

the presence of solid GNP nano-additive in the EO fluid. Consequently, increasing the GNP nano-additive concentration results in higher nanofluid viscosity. However, it's important to note that the dynamic viscosity does not always increase significantly with concentration. For instance, in Fig. 5.11 (c) and (d), the increase in dynamic viscosity is negligible as relative to lower temperature of 40°C.

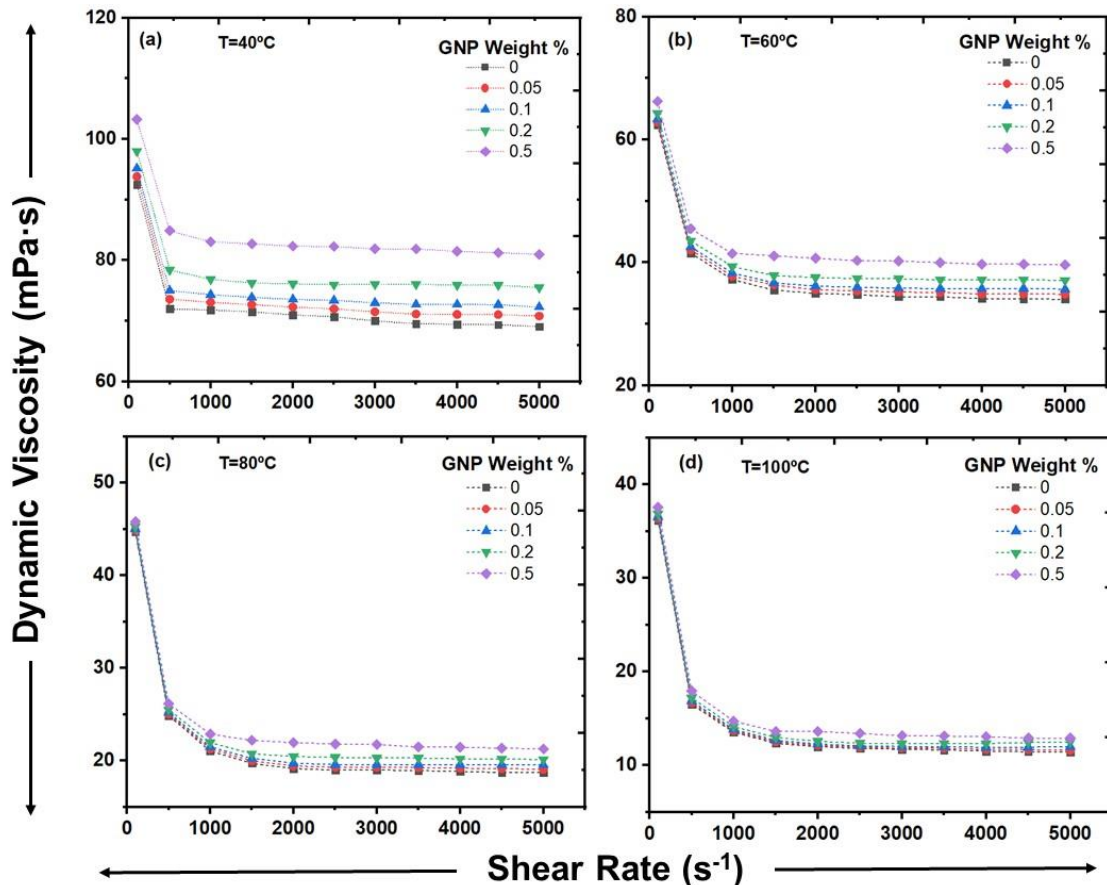


**Fig. 5.17 (a-d):** Effect of shear rate on dynamic viscosity of GNP/EO nanofluids at different mass fraction.

Fig. 5.19 depicts the influence of temperature on the dynamic viscosity of pure EO and GNP/EO nanofluids with varying nano-additive GNP weight %. This analysis is conducted at constant shear rates of 500 s<sup>-1</sup> and 5000 s<sup>-1</sup>. As the temperature rises from 40°C to 100°C, the dynamic viscosity decreases for both EO fluids and GNP/EO nanofluids. For instance, at a shear rate of 500 s<sup>-1</sup>, the GNP/EO nanofluid with a 0.5 weight% GNP concentration shows a viscosity of 84 mPa·s at 40°C, which decreases to 18 mPa·s at 100°C. Similar trends are observed for other nano-additive GNP weight %. These observations can be attributed to a decrease in intermolecular adhesion forces as temperature rises. Moreover, the effect of solid nano-additive GNP concentration on

dynamic viscosity is more prominent at lower temperatures. However, this influence becomes less significant as the temperature increases.

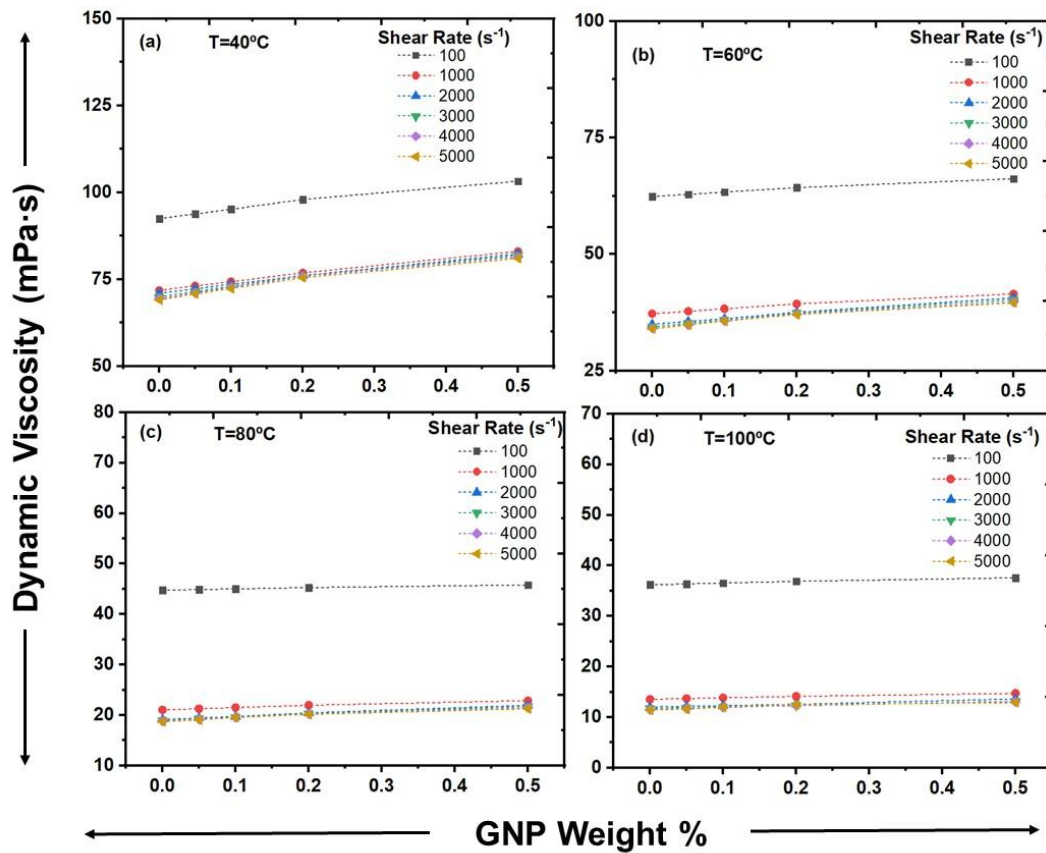


Fig. 5.18 (a-d): Effect of solid mass fractions on dynamic viscosity of GNP/EO nanofluids at different shear rates.

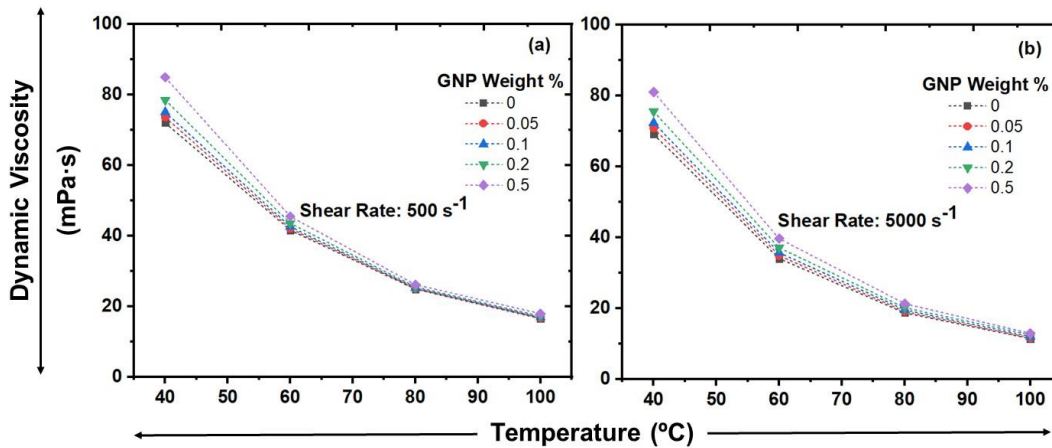
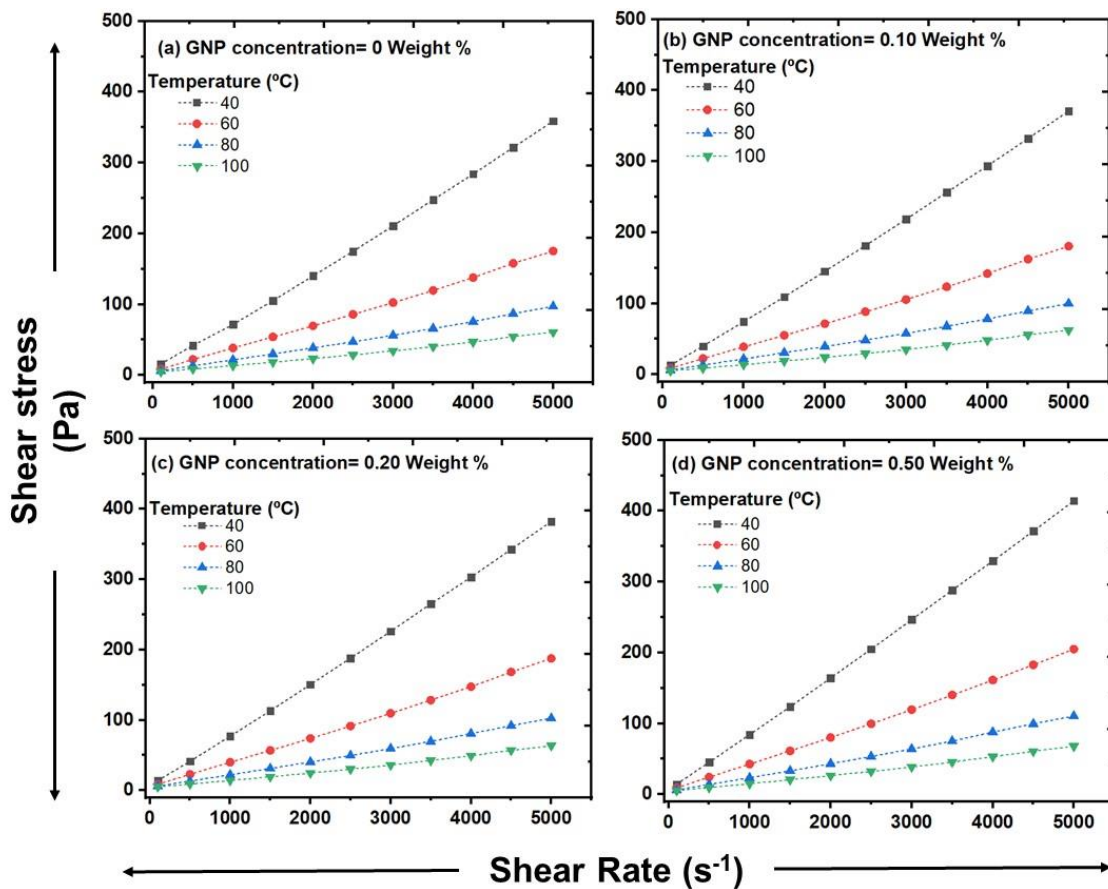


Fig. 5.19 (a-b): Effect of temperature on the dynamic viscosity of GNP/EO nanofluids at different solid mass fractions.

In Fig. 5.20 (a-d), the correlation between shear rate & shear stress of GNP/EO nanofluid is depicted at different temperatures for various GNP weight % (0.0, 0.05, 0.1,

0.2, and 0.5). The figures demonstrate that shear stress increases as shear rate increases across all temperatures. To determine the flow behaviour of the fluid, whether it follows newtonian flow or non-newtonian flow, the Ostwald-de-Waele (OdW) model is employed using Equation (1) as discussed in introduction part of chapter 1 [1-3]. In this analysis, fitting of power law curves was applied to the shear stress vs. shear rate curve to find the values of consistency index ( $m$ ) and power law index ( $n$ ). The obtained values of  $m$  and  $n$  are displayed in Table 5.3.



**Fig. 5.20 (a-d):** Shear stress vs. shear rate at various temperature for GNP/EO nanofluids.

As shown in Fig. 5.21, the values of power law index ( $n$ ) are close to or equal to one at 40°C for all nano-additive GNP weight % and temperature ranges of the nanofluids, indicating a newtonian fluid flow behaviour. At 100°C, the values of  $n$  for all nano-additive GNP weight % of the nanofluids are less than 1, suggesting a pseudo plastic non-newtonian fluid flow behaviour. At 60°C and 80°C temperatures, with increasing nano-additive GNP concentration in EO, different flow characteristics are observed. At lower concentration 0.05 weight %, EO and GNP/EO nanofluids show pseudo plastic non-

newtonian fluid behaviour. Above 0.05 weight % concentration, GNP/EO nanofluid show newtonian fluid behaviour. This observation suggests that at higher temperatures of 80°C and 100°C, GNP/EO nanofluids shows different flow behaviours than lower temperatures 40°C and 60°C depending on nano-additive GNP concentration in base fluid. This may help in designing the GNP/EO nanofluid as per flow behaviour requirement in different type of EO applications.

**Table 5.3:** The power law index (n) and consistency index (m) values of GNP/EO nanofluids.

Temperature (°C)	Indexes	GNP concentration (Weight %)				
		0	0.05	0.1	0.2	0.5
40	m	66	66	68	74	85
	n	1.0083	1.0107	1.0081	1.0036	0.9965
60	m	43	42	42	42	42
	n	0.9755	0.9783	0.9810	0.9862	0.9953
80	m	26	25	25	24	23
	n	0.9652	0.9691	0.9728	0.9800	0.9929
100	m	14	15	15	15	16
	n	0.9779	0.9775	0.9771	0.9763	0.9749

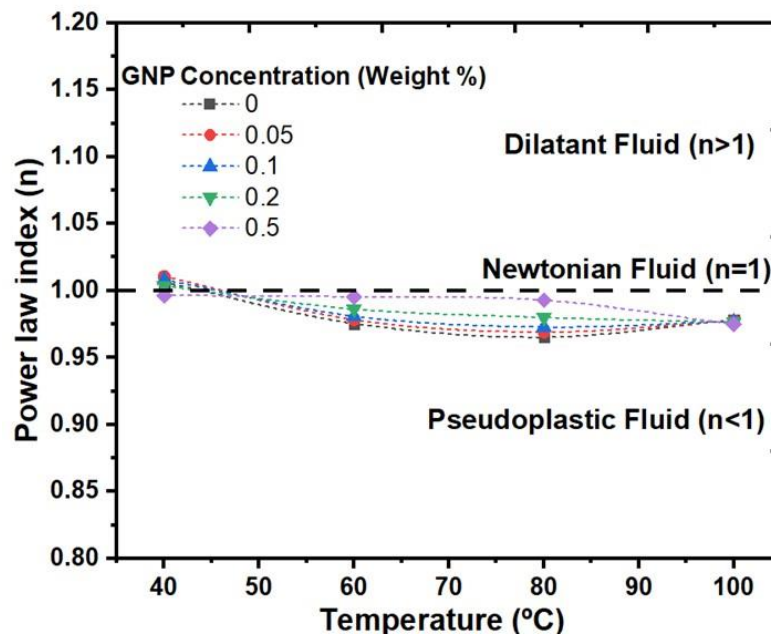


**Fig. 5.21:** Power law index for different solid mass fractions and temperature for GNP/EO nanofluids.

Furthermore, Fig. 5.22 depicts the relationship between the nanofluids' temperature & the consistency index (m) for different GNP weight%. The results clearly demonstrate m value declines with increasing temperature. This indicates that as the temperature rises, the fluid's mobility decreases, resulting in reduced flow resistance. It is noteworthy that the

consistency index does not change much with the GNP concentration at higher temperatures. This observation confirms that higher GNP concentrations in the base fluid do not substantially increase resistance to fluid flow.

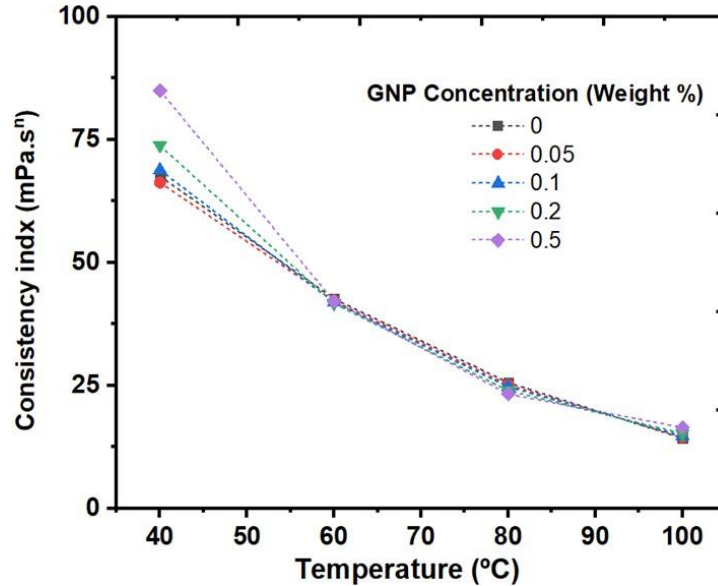


**Fig. 5.22:** Consistency index for different solid mass fractions and temperatures for GNP/EO nanofluids.

#### 5.4.2: Thermal conductivity characteristics of GNP/EO nanofluids

In Fig. 5.23 (a), the thermal conductivity of pure EO and GNP/EO nanofluid is shown for GNP concentration over a temperature: 30°C to 70°C. The data reveal that the thermal conductivity improves with an increase in the GNP concentration. Moreover, at higher ZnO concentrations, thermal conductivity exhibits a steeper slope, indicating a more pronounced enhancement. This increased thermal conductivity is attributed to higher heat conductivity of GNP incorporated into the EO fluid. It is noteworthy to notice, thermal conductivity of both EO fluid and the GNP/EO nanofluid with a 0.05 weight % GNP concentration diminish as the temperature increases. However, a thermal conductivity reversal behaviour is observed at a GNP concentration above 0.1 weight% in the BO. In this case, the thermal conductivity of GNP/EO nanofluids increases with rising temperature. This is explained by the increased interaction and spread of GNP particles within the EO fluid at higher temperatures. These changes are driven by the energy transfer between the layers of the nanofluid, resulting in enhanced heat transfer capabilities of the nanofluids [4-6]. Overall, the finding shows that GNP/EO nanofluids have enhanced thermal conductivity relative to the pure EO fluid.

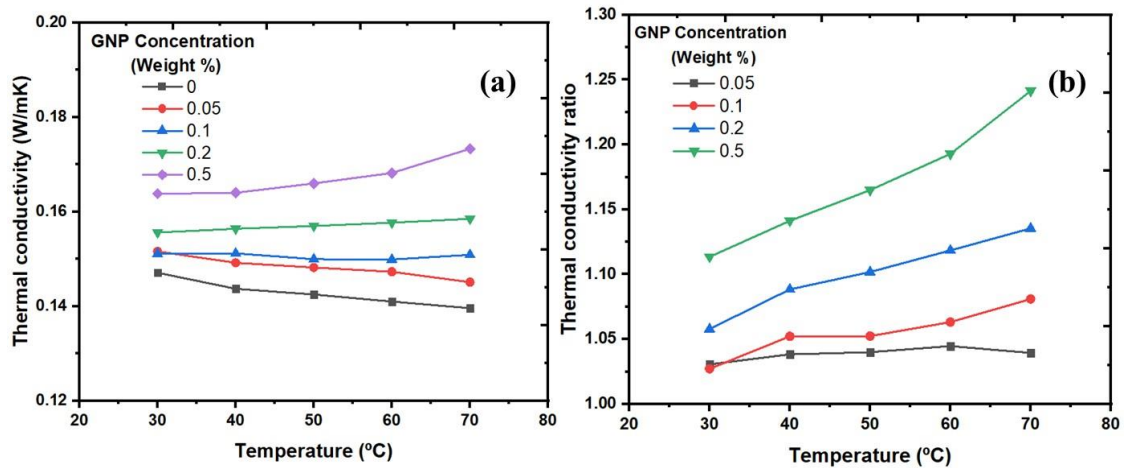


**Fig. 5.23:** (a) Thermal conductivity of GNP/EO nanofluids, and (b) thermal conductivity ratio of GNP/EO nanofluids.

The thermal conductivity ratio of the GNP/EO nanofluid relative to the EO base fluid is shown in Fig. 5.23 (b). The ratio increases with rising temperature. At low GNP weight %, there are minimal increases in thermal conductivity because of lower concentration of GNP in the fluid. However, as the GNP concentration increases, the number of nanoparticles & their collisions also increases, resulting in effective heat transfer between fluid layers [7, 8]. This results in greater thermal conductivity values for the GNP/EO nanofluid relative to the base EO fluid. In our study, the thermal conductivity of the GNP/EO nanofluid increased by 24% at 70°C for a GNP weight % of 0.5%. This significant enhancement demonstrates the capability of GNP/EO nanofluids to enhance heat transfer performance in various EO applications.

## 5.5: EO-based nanofluid containing MWCNT nano-additives (MWCNT/EO nanofluids)

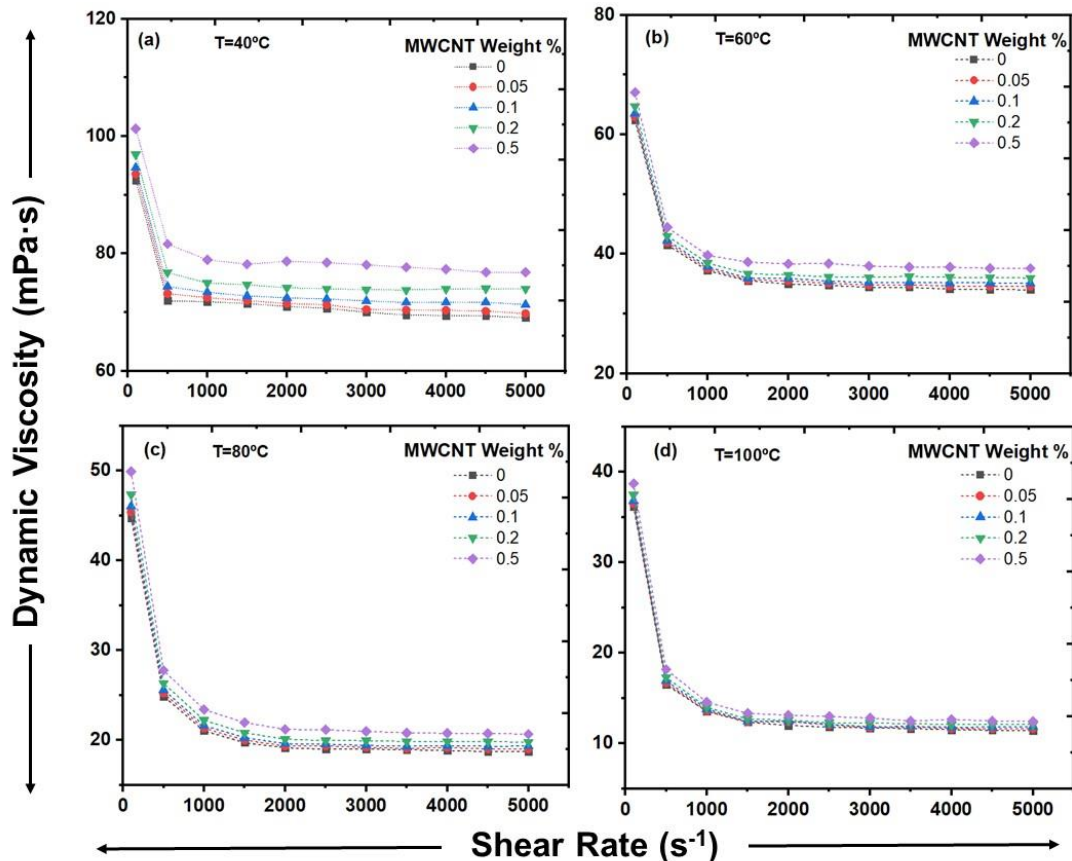
In this study, a comprehensive rheological investigation was carried out to assess the dynamic viscosity of both pure EO and MWCNT/EO nanofluids under different MWCNT nano-additive concentrations, shear rates, and temperature conditions. The main focus was to understand the influence of MWCNT weight % and temperature on the dynamic viscosity and thermal conductivity of MWCNT/EO nanofluids. The obtained results shed light on the potential applications of MWCNT/EO nanofluids as efficient EOs.

### 5.5.1: Flow characteristics of MWCNT/EO nanofluids using rheometry

Fig. 5.24 exhibits the impact of shear rate on the dynamic viscosity of MWCNT/EO nanofluids at different MWCNT weight % and temperatures: 40°C to 100°C. The findings indicate that the dynamic viscosity of both MWCNT/EO nanofluids and pure EO decreases with increasing shear rates at all measured temperature range for all nano-additive concentrations. This shows initial shear thinning behaviour of non-newtonian fluid. At higher shear rates and at all temperatures, all fluids exhibit linear behaviour indicating newtonian fluid characteristic i.e., fluids have a constant viscosity regardless of the shear rates applied. The experimental findings suggest a newtonian fluid behaviour for both MWCNT/EO nanofluids and pure EO at higher shear rates at any temperature within the experimental range. However, at higher shear rates and higher temperature, nanofluids with higher MWCNT weight % exhibit a slight pseudoplastic i.e., shear-thinning behaviour relative to nanofluids with lower MWCNT weight %. This observation suggests that increased MWCNT concentration, represented by weight %, has a notable impact on enhancing shear thinning in both MWCNT/EO nanofluids and pure EO.

Fig. 5.25 presents the effect of MWCNT weight% on dynamic viscosity of constantly-temperated nanofluids. The MWCNT concentration has a significant effect on the dynamic viscosity within the shear rate range of 100 to 5000  $s^{-1}$  at 40°C, 60 °C and 80°C temperatures. At these temperatures dynamic viscosity of all nanofluids increases slightly with increasing MWCNT nano-additive concentration. However, at higher temperatures i.e., 100°C, rate of increase in dynamic viscosity with increasing MWCNT nano-additive concentration became very less at all shear rates. At lower temperatures (40°C and 60°C), increased dynamic viscosity of nanofluids attributed to the enhanced

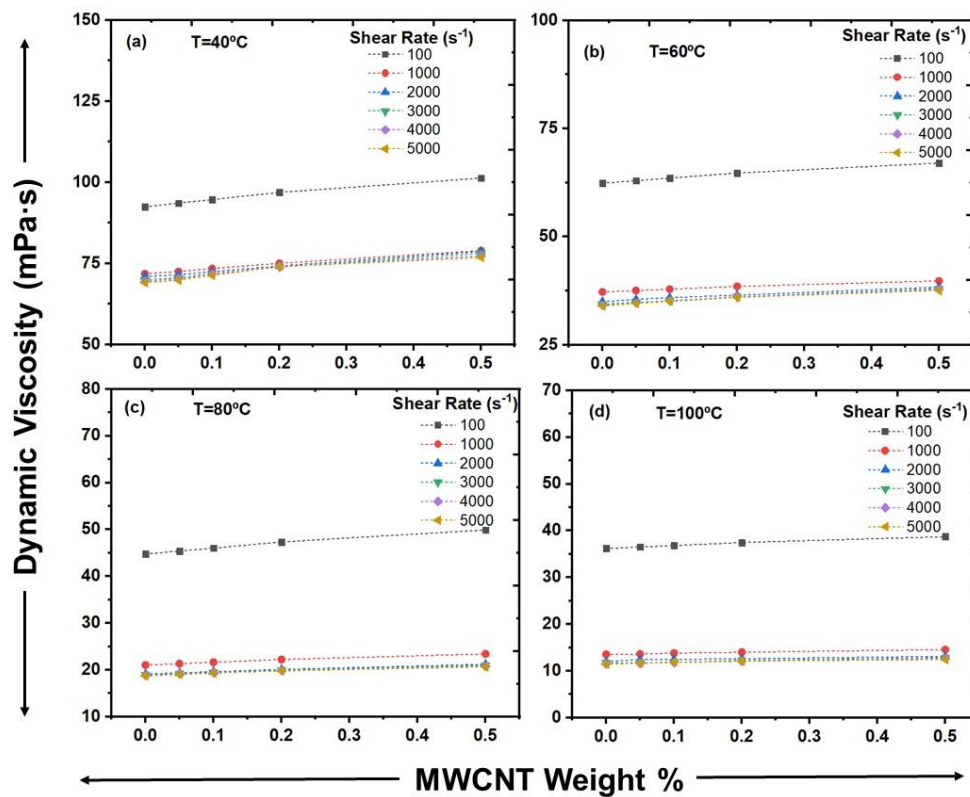
resistance to flow depicted by the presence of solid MWCNT nano-additive in the EO fluid. Consequently, increasing the MWCNT nano-additive concentration results in higher nanofluid viscosity. However, it's important to note that the dynamic viscosity does not always increase significantly with concentration. For instance, in Fig. 5.25 (d), the increase in dynamic viscosity is negligible as relative to lower temperature of 40°C.



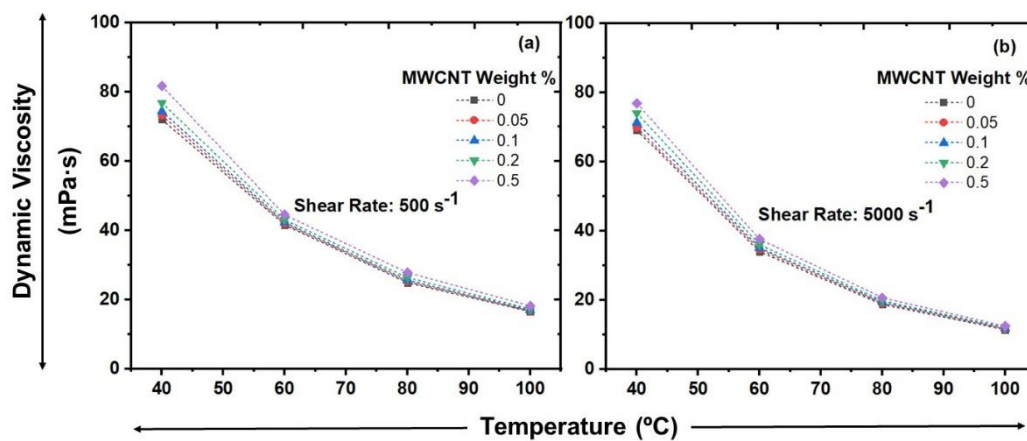
**Fig. 5.24 (a-d):** Effect of shear rate on dynamic viscosity of MWCNT/EO nanofluids at different mass fraction.

Fig. 5.26 depicts the influence of temperature on the dynamic viscosity of pure EO and MWCNT/EO nanofluids with varying nano-additive MWCNT weight %. This analysis is conducted at constant shear rates of 500 s<sup>-1</sup> and 5000 s<sup>-1</sup>. As the temperature rises from 40°C to 100°C, the dynamic viscosity decreases for both EO fluids and MWCNT/EO nanofluids. For instance, at a shear rate of 5000 s<sup>-1</sup>, the MWCNT/EO nanofluid with a 0.5 weight% MWCNT concentration shows a viscosity of 77 mPa·s at 40°C, which decreases to 12 mPa·s at 100°C. Similar trends are observed for other nano-additive MWCNT weight %. These observations can be attributed to a decrease in intermolecular adhesion forces as temperature rises. Moreover, the effect of solid nano-additive MWCNT concentration on

dynamic viscosity is more prominent at lower temperatures. However, this influence becomes less significant as the temperature increases.



**Fig. 5.25 (a-d):** Effect of solid mass fractions on dynamic viscosity of MWCNT/EO nanofluids at different shear rates.



**Fig. 5.26 (a-b):** Effect of temperature on the dynamic viscosity of MWCNT/EO nanofluids at different solid mass fractions.

In Fig. 5.27 (a-d), the correlation between shear rate & shear stress of MWCNT/EO nanofluid is depicted at different temperatures for various MWCNT weight % (0.0, 0.05, 0.1, 0.2, and 0.5). The figures demonstrate that shear stress increases as shear rate increases

across all temperatures. To determine the flow behaviour of the fluid, whether it follows newtonian flow or non-newtonian flow, the Ostwald-de-Waele (OdW) model is employed using Equation (1) as discussed in introduction part of chapter 1 [1-3]. In this analysis, fitting of power law curves was applied to the shear stress vs. shear rate curve to find the values of consistency index ( $m$ ) and power law index ( $n$ ). The obtained values of  $m$  and  $n$  are displayed in Table 5.4.

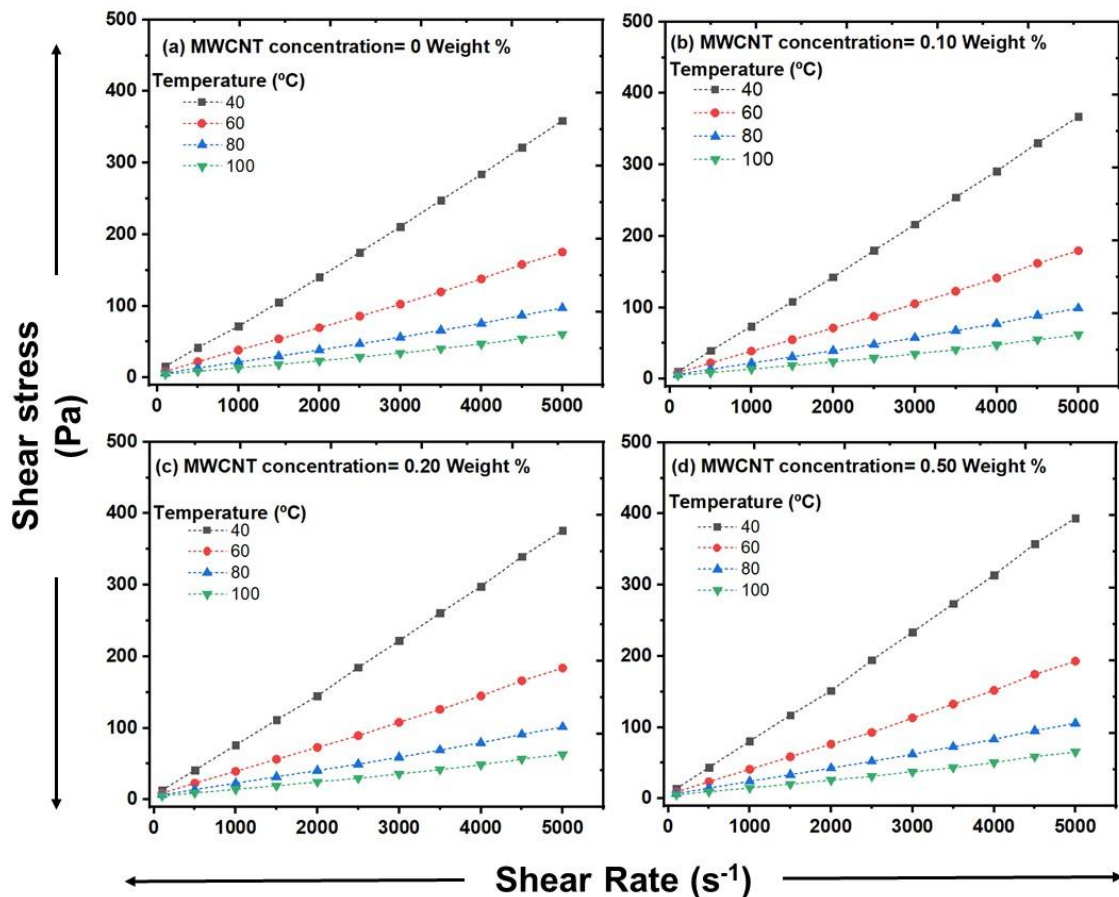


**Fig. 5.27 (a-d):** Shear stress vs. shear rate at various temperature for MWCNT/EO nanofluids.

As shown in Fig. 5.28, the values of power law index ( $n$ ) are close to or equal to one at 40°C for all nano-additive MWCNT weight % and temperature ranges of the nanofluids, indicating a newtonian fluid flow behaviour. The values of  $n$  for all nano-additive MWCNT weight % and temperatures (80°C and 100°C) of the nanofluids are less than 1, suggesting a pseudo plastic non-newtonian fluid flow behaviour. At 60°C with increasing nano-additive MWCNT concentration in EO, different flow characteristics are observed. At lower concentration 0.05 weight %, EO and MWCNT/EO nanofluids show

pseudo plastic non-newtonian fluid behaviour. Above 0.05 weight % concentration, MWCNT/EO nanofluid show newtonian fluid behaviour. This observation suggests that at higher temperatures of 80°C and 100°C, MWCNT/EO nanofluids shows different flow behaviours than lower temperatures 40°C and 60°C depending on nano-additive MWCNT concentration in base fluid. This may help in designing the MWCNT/EO nanofluid as per flow behaviour requirement in different type of EO applications.

**Table 5.4:** The power law index (n) and consistency index (m) values of MWCNT/EO nano-fluids.

Temperature (°C)	Indexes	MWCNT concentration (Weight %)				
		0	0.05	0.1	0.2	0.5
40	m	66	65	65	68	73
	n	1.0083	1.0119	1.0133	1.0111	1.0083
60	m	43	43	42	42	42
	n	0.9755	0.9754	0.9800	0.9828	0.9899
80	m	26	27	28	29	33
	n	0.9652	0.9618	0.9581	0.9554	0.9456
100	m	14	15	16	16	18
	n	0.9779	0.9721	0.9699	0.9663	0.9583

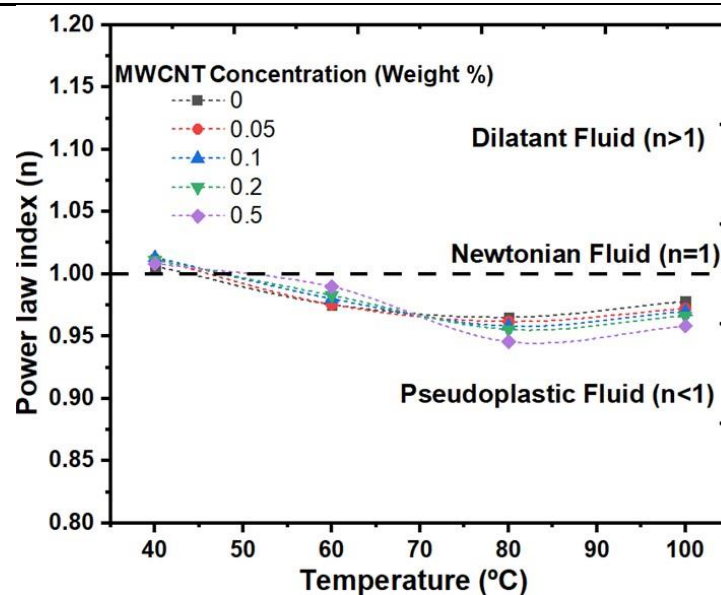


**Fig. 5.28:** Power law index for different solid mass fractions and temperature for MWCNT/EO nanofluids.

Furthermore, Fig. 5.29 depicts the relationship between the nanofluids' temperature & the consistency index (m) for different MWCNT weight%. The results clearly demonstrate m value declines with increasing temperature. This indicates that as the temperature rises, the fluid's mobility decreases, resulting in reduced flow resistance. It is noteworthy that the consistency index does not change much with the MWCNT

concentration at higher temperatures. This observation confirms that higher MWCNT concentrations in the base fluid do not substantially increase resistance to fluid flow.

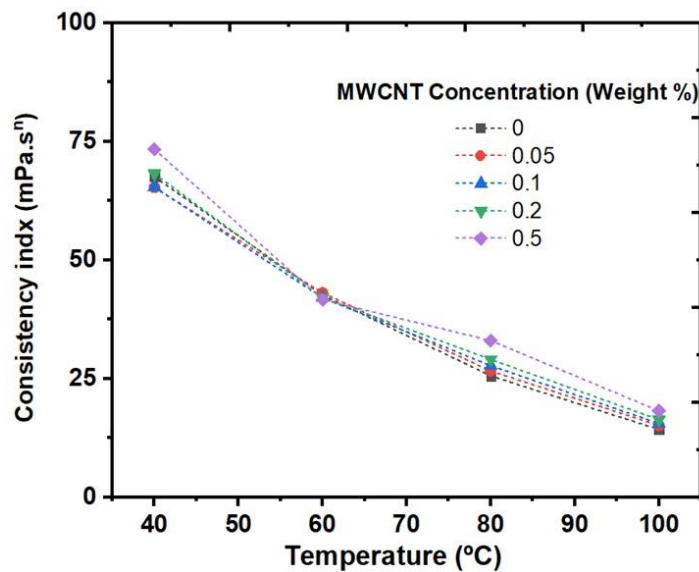


**Fig. 5.29:** Consistency index for different solid mass fractions and temperatures for MWCNT/EO nanofluids.

### 5.5.2: Thermal conductivity characteristics of MWCNT/EO nanofluids

In Fig. 5.30 (a), the thermal conductivity of pure EO and MWCNT/EO nanofluid is shown for MWCNT concentration over a temperature: 30°C to 70°C. The data reveal that the thermal conductivity improves with an increase in the MWCNT concentration. Moreover, at higher MWCNT concentrations, thermal conductivity exhibits a steeper slope, indicating a more pronounced enhancement. This increased thermal conductivity is attributed to higher heat conductivity of MWCNT incorporated into the EO fluid. It is noteworthy to notice, thermal conductivity of both EO fluid and the MWCNT/EO nanofluid with a 0.05 weight % MWCNT concentration diminish as the temperature increases. However, a thermal conductivity reversal behaviour is observed at a MWCNT concentration above 0.1 weight% in the BO. In this case, the thermal conductivity of MWCNT/EO nanofluids increases with rising temperature. This is explained by the increased interaction and spread of MWCNT particles within the EO fluid at higher temperatures. These changes are driven by the energy transfer between the layers of the nanofluid, resulting in enhanced heat transfer capabilities of the nanofluids [4-6]. Overall, the finding shows that MWCNT/EO nanofluids have enhanced thermal conductivity relative to the pure EO fluid.

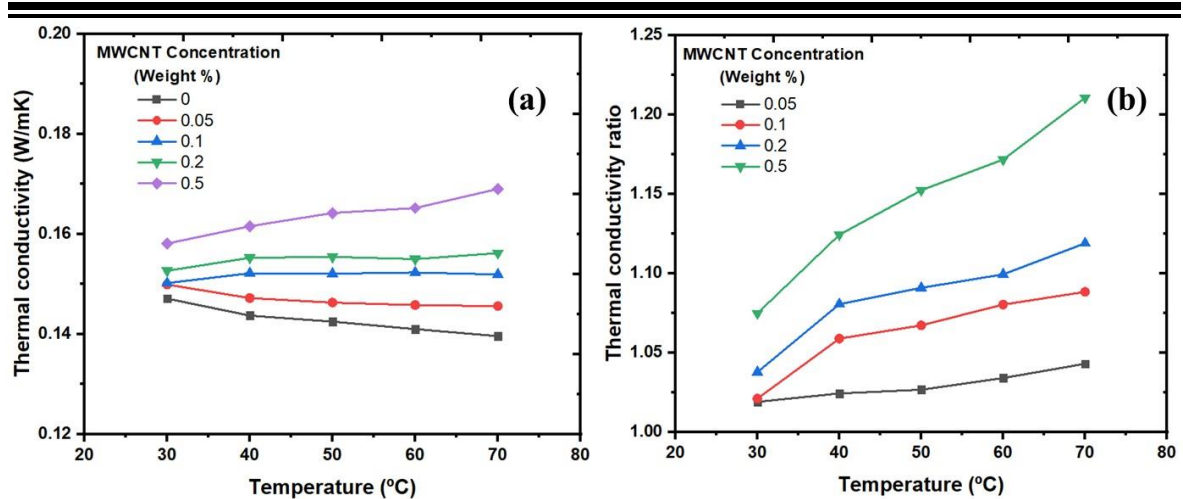


**Fig. 5.30:** (a) Thermal conductivity of MWCNT/EO nanofluids, and (b) thermal conductivity ratio of MWCNT/EO nanofluids.

The thermal conductivity ratio of the MWCNT/EO nanofluid relative to the EO base fluid is shown in Fig. 5.30 (b). The ratio increases with rising temperature. At low MWCNT weight %, there are minimal increases in thermal conductivity because of lower concentration of MWCNT in the fluid. However, as the MWCNT concentration increases, the number of nanoparticles & their collisions also increases, resulting in effective heat transfer between fluid layers [7, 8]. This results in greater thermal conductivity values for the MWCNT/EO nanofluid relative to the base EO fluid. In our study, the thermal conductivity of the MWCNT/EO nanofluid increased by 21% at 70°C for a MWCNT weight % of 0.5%. This significant enhancement demonstrates the capability of MWCNT/EO nanofluids for improving heat transfer performance in various EO applications

## 5.6: Results and discussion

To assess the enhancement in the flow and thermal conductivity properties of the EO dispersed with different nano-additives (Al<sub>2</sub>O<sub>3</sub>, ZnO, GNP, and MWCNT), a series of experiments were performed. The overall results acquired through the experiments were furnished below.

As per the Ostwald-de-Waele (OdW) model, pure EO and EO-based nanofluids with different nano-additives were evaluated for finding the fluid flow characteristics under variable shear stress, temperature and nano-additives concentration conditions [1-3]. All EO and EO-based nanofluids flow behaviour are represented in Table 5.5.

All the EO-based nanofluids exhibit Newtonian fluid flow behaviour at 40°C. All the EO-based nanofluids exhibit pseudoplastic non-newtonian fluid flow characteristics at 100°C, which indicates fluids viscosity, or the flow resistance, decreases as the force or shear rate increases. In other words, the more you stir or squeeze, the easier it flows. However, if you stop applying the force, it thickens up again over time [9-11]. As shown in Table 5.5, the EO-based nanofluids exhibits various fluid flow behaviour at 60°C and 80°C temperatures depending on nature of nano-additives. MWCNT nano-additive can easily change the EO newtonian behaviour to pseudoplastic non-newtonian fluid flow behaviour at higher concentrations and temperatures. While, GNP nano-additive maintain the EO newtonian behaviour at higher concentrations and up to 80°C temperature. Al<sub>2</sub>O<sub>3</sub> and ZnO nano-additives at higher concentrations maintains newtonian fluid behaviour up to 60°C temperature.

Pure EO and EO-based nanofluids with different nano-additives were evaluated for measuring the thermal conductivity characteristics under different temperature and nano-additives concentration conditions. The thermal conductivity enhancement of nanofluids in percentage at temperature shown in Table 5.6 in relative to pure EO. Carbon based nano-additives (GNP and MWCNT) increases thermal conductivity of base fluid greater than the metal-oxide based nano-additives (Al<sub>2</sub>O<sub>3</sub> and ZnO) [12]. GNP nano-additive shows maximum thermal conductivity enhancement of 24% at 0.5 weight % concentration at 70°C. GNP at 0.5 weight % nano-additives concentration, increases thermal conductivity of base EO fluid by more than 10% for all temperature range measured. MWCNT at 0.5 weight % nano-additives concentration, increases thermal conductivity of base EO fluid by more than 10% above 30°C temperature.

Table 5.5: Flow behaviour of EO-based nanofluids

Nanofluid	Nano-additive weight %	Temperature (°C)			
		40	60	80	100
EO	Pure	N	PP	PP	PP
$Al_2O_3$ /EO	0.05	N	PP	PP	PP
	0.1	N	N	PP	PP
	0.2	N	N	PP	PP
	0.5	N	N	PP	PP
ZnO/EO	0.05	N	PP	PP	PP
	0.1	N	N	PP	PP
	0.2	N	N	PP	PP
	0.5	N	N	PP	PP
GNP/EO	0.05	N	PP	PP	PP
	0.1	N	N	PP	PP
	0.2	N	N	N	PP
	0.5	N	N	N	PP
MWCNT/EO	0.05	N	N	PP	PP
	0.1	N	PP	PP	PP
	0.2	N	PP	PP	PP
	0.5	N	PP	PP	PP

*PP: Pseudo plastic non-newtonian fluid, D: Dilatant non-newtonian fluid, N: Newtonian fluid*

GNP and MWCNT exhibit higher thermal conductivity relative to metal-oxide nano-additives due to their unique structural and material properties. Graphene is a two-dimensional material composed of a single layer of carbon atoms arranged in a hexagonal lattice, while CNTs are cylindrical structures made of rolled-up graphene sheets. These carbon-based nanomaterials possess excellent thermal conductivity because of their highly ordered atomic structures and strong covalent bonding between carbon atoms. This allows them to efficiently transfer heat through phonon vibrations along their carbon-carbon bonds. Additionally, carbon-based nanomaterials like GNP and MWCNT have higher aspect ratios and larger surface areas, which facilitate better dispersion and interaction within the fluid. This enhanced dispersion allows for more effective thermal conduction pathways throughout the fluid, further increasing its overall thermal conductivity [13, 14].

In contrast, metal-oxide nano-additives (Al<sub>2</sub>O<sub>3</sub> and ZnO) typically have lower thermal conductivity because of their crystalline structures and the presence of lattice defects, grain boundaries, and phonon scattering sites. These factors hinder the efficient transfer of heat through the material, resulting in lower thermal conductivity relative to carbon-based nanomaterials [5, 15, 16].

**Table 5.6:** Enhancement of thermal conductivity (%) of EO-based nanofluids.

Nanofluid	Nano-additive weight %	Temperature (°C)				
		30	40	50	60	70
Al <sub>2</sub> O <sub>3</sub> /EO	0.05	0.5	1.1	1.6	2.1	3.1
	0.1	1.5	5.4	6.2	7.5	8.3
	0.2	2.4	6.6	7.6	8.9	<b>10.5</b>
	0.5	5.3	9.8	<b>12.6</b>	<b>15.3</b>	<b>18.4</b>
ZnO/EO	0.05	0.2	1.3	1.9	2.2	3.0
	0.1	0.9	2.7	3.6	4.7	6.2
	0.2	1.7	5.4	6.8	7.8	9.1
	0.5	3.2	6.6	9.1	<b>11.1</b>	<b>13.0</b>
GNP/EO	0.05	3.1	3.8	4.0	4.5	3.9
	0.1	2.7	5.2	5.2	6.3	8.1
	0.2	5.8	8.8	<b>10.2</b>	<b>11.8</b>	<b>13.5</b>
	0.5	<b>11.4</b>	<b>14.1</b>	<b>16.5</b>	<b>19.3</b>	<b>24.1</b>
MWCNT/EO	0.05	1.9	2.4	2.7	3.4	4.3
	0.1	2.1	5.9	6.7	8.0	8.8
	0.2	3.8	8.1	9.1	9.9	<b>11.9</b>
	0.5	7.5	<b>12.4</b>	<b>15.2</b>	<b>17.2</b>	<b>21.1</b>

In metal-oxide nano-additives, Al<sub>2</sub>O<sub>3</sub> nano-additive exhibits good thermal conductivity enhancement relative to ZnO nano-additive. Al<sub>2</sub>O<sub>3</sub> nano-additive possesses a higher thermal conductivity because of its dense crystalline structure and strong atomic bonding, which allows heat to propagate more efficiently through the material.

Overall, the unique structural and material properties of versatile GNP and MWCNT contribute to their superior ability to enhance the thermal conductivity of fluids relative to nano-additives: Al<sub>2</sub>O<sub>3</sub> and ZnO.

## 5.7: Chapter Conclusion

The present study investigates the flow and thermal conductivity behaviour of EO-based nanofluids with different nano-additive concentrations at 0.05, 0.1, 0.2, and 0.5 weight %. Using an advanced ultrasonically-assisted method, the Al<sub>2</sub>O<sub>3</sub>/EO, ZnO/EO, GNP/EO and MWCNT/EO nanofluids were successfully stabilized. Rheological investigations were carried out at various shear rates and temperatures, revealing a different flow behaviour across all samples. Thermal conductivity study was carried out to understand nano-additive effect on base EO across the temperature range. The study contributes to the existing knowledge on thermophysical properties of EO and sets the stage for further advancements in the field. The following are the key findings of the work:

1. The dynamic viscosity of both the EO fluid and EO-based nanofluids exhibited a reduction at the initial increase in shear rate of 100 s<sup>-1</sup> and at all temperatures. Furthermore, the viscosity remained stable as the shear rate and temperature was further increased across all temperatures studied.
2. With increasing temperature from 40°C to 100°C, the dynamic viscosity of all nanofluids remained stable across all nano-additives concentrations at higher shear rates. At lower temperatures of 40°C and 60 °C, the nano-additives weight% and type of nano-additives have a significant impact on viscosity, while its influence diminishes as the temperature rises.
3. The power law index (n) values for all weight % of any nano-additives based EO nanofluids, obtained at 40°C temperature, are close to or equal to 1. This observation confirms the newtonian flow behaviour of all nanofluid at 40°C. The power law index (n) values for all weight % of any nano-additives based EO nanofluids, obtained at 100°C temperature, are less than 1. This observation confirms the pseudoplastic non-newtonian fluid flow behaviour of all nanofluid at 100°C. At 60°C and 80°C temperatures, all nano-fluids show different flow behaviour based on nano-additives nature and concentrations.
4. The concentration of nano-additives significantly influences the dynamic viscosity and thermal conductivity behaviour of EO-based nanofluids. The interactions between nano-additives and EO play a crucial role in enhancing the heat conduction and transfer capabilities of EO-based nanofluids relative to the pure EO. In fact, the thermal conductivity was observed to increase by 24% in the best-case scenario at

70°C for a GNP/EO nanofluid with a concentration of 0.5 weight%. Carbon based nano-additives GNP and MWCNT have higher impact on increasing thermal conductivity of base EO fluid as relative to metal oxide-based nano-additives i.e.,  $Al_2O_3$  and ZnO.

5. For consistent lubrication in engine components applications where newtonian fluid with high thermal conductivity is desirable, 0.5 weight % GNP/EO nanofluid is suitable nanofluid.
6. Pseudoplastic fluids like grease, adjust viscosity under shear stress, providing both lubrication and sealing properties, ideal for high-pressure and temperature environments within engines. For these applications, 0.5 weight % MWCNT/EO is suitable nanofluid with approximate 21% thermal conductivity improvement as relative to EO base fluid.

The present findings strongly suggest that GNP/EO nanofluids hold substantial promise as valuable and cost-effective materials for diverse lubrication and heat transfer applications in automotive industry. However, we recognize the need for further exploration and meticulous calculations of heat transfer coefficients in practical heat transfer contexts.

## 5.8: References

- [1] Afrand, Masoud, Davood Toghraie, and Behrooz Ruhani, Effects of temperature and nano-additives concentration on rheological behavior of  $Fe_3O_4$ -Ag/EG hybrid nanofluid: an experimental study, *Experimental Thermal and Fluid Science*, 77 (2016) 38-44.
- [2] Bharath, Bhavin K., and V. Arul Mozhi Selvan, An experimental investigation on rheological and heat transfer performance of hybrid nanolubricant and its effect on the vibration and noise characteristics of an automotive spark-ignition engine, *International Journal of Thermophysics*, 42 (2021) 1-30.
- [3] Vora, Vishal, Rakesh K. Sharma, and D. P. Bharambe, Investigation of rheological and thermal conductivity properties of castor oil nanofluids containing graphene nanoplatelets, *International Journal of Thermophysics*, 44.10 (2023) 155.
- [4] Godson, Lazarus, B. Raja, D. Mohan Lal, and S. E. A. Wongwises, Enhancement of heat transfer using nanofluids-an overview, *Renewable and sustainable energy reviews*, 14 (2010) 629-641.
- [5] Lenin, Ramanujam, Pattayil Alias Joy, and Chandan Bera, A review of the recent progress on thermal conductivity of nanofluid, *Journal of Molecular Liquids*, 338 (2021) 116929.
- [6] Machrafi, Hatim, and Georgy Lebon, The role of several heat transfer mechanisms on the enhancement of thermal conductivity in nanofluids, *Continuum Mechanics and Thermodynamics*, 28 (2016) 1461-1475.
- [7] Kakaç, Sadik, and Anchasa Pramuanjaroenkij, Review of convective heat transfer enhancement with nanofluids, *International journal of heat and mass transfer*, 52 (2009): 3187-3196
- [8] Amani, Mohammad, Pouria Amani, Mehdi Bahiraei, Mohammad Ghalambaz, Goodarz Ahmadi, Lian-Ping Wang, Somchai Wongwises, and Omid Mahian, Latest developments in nanofluid flow and heat transfer between parallel surfaces: A critical review, *Advances in Colloid and Interface Science*, 294 (2021) 102450.
- [9] Cross, Malcolm M, Rheology of non-Newtonian fluids: a new flow equation for pseudoplastic systems, *Journal of colloid science*, 20 (1965): 417-437.

- [10] Guedda, M., and R. Kersner, Non-Newtonian pseudoplastic fluids: Analytical results and exact solutions, *International Journal of Non-Linear Mechanics*, 46 (2011) 949-957.
- [11] Liu, Shengna, Xuehui Chen, and Liancun Zheng, Heat transfer of pseudo-plastic fluid in shear flow with field correlation, *Journal of the Taiwan Institute of Chemical Engineers*, 146 (2023) 104874.
- [12] Rajamony, R.K., Paw, J.K.S., Pandey, A.K., Tak, Y.C., Pasupuleti, J., Tiong, S.K., Yusaf, T., Samykano, M., Sofiah, A.G.N., Kalidasan, B. and Ahmed, O.A., Energizing the thermophysical properties of phase change material using carbon-based nano additives for sustainable thermal energy storage application in photovoltaic thermal systems, *Materials Today Sustainability*, 25 (2024) 100658.
- [13] Younes, Hammad, Mingyang Mao, SM Sohel Murshed, Ding Lou, Haiping Hong, and G. P. Peterson, Nanofluids: Key parameters to enhance thermal conductivity and its applications, *Applied Thermal Engineering*, 207 (2022) 118202.
- [14] Jebasingh, B. Eanest, and A. Valan Arasu, A comprehensive review on latent heat and thermal conductivity of nanoparticle dispersed phase change material for low-temperature applications, *Energy Storage Materials*, 24 (2020) 52-74.
- [15] Wanatasanapan, V. Vicki, M. Z. Abdullah, and P. Gunnasegaran, Effect of TiO<sub>2</sub>-Al<sub>2</sub>O<sub>3</sub> nanoparticle mixing ratio on the thermal conductivity, rheological properties, and dynamic viscosity of water-based hybrid nanofluid, *Journal of Materials Research and Technology*, 9 (2020) 13781-13792.
- [16] Apmann, Kevin, Ryan Fulmer, Alberto Soto, and Saeid Vafaei, Thermal conductivity and viscosity: Review and optimization of effects of nanoparticles, *Materials*, 14 (2021) 1291.